NASA TECHNICAL NOTE

NASA TN D-5200

NASA TN D-5200

COMPUTER SIMULATION OF A CYLINDRICAL GALAXY

by Frank Hohl

Langley Research Center
Langley Station, Hampton, Va.

NATIONAL AERONAUTICS AND SPACE ADMINISTRATION • WASHINGTON, D. C. • MAY 1969

NASA TN D-5200

COMPUTER SIMULATION OF A CYLINDRICAL GALAXY

By Frank Hohl

Langley Research Center
Langley Station, Hampton, Va.

NATIONAL AERONAUTICS AND SPACE ADMINISTRATION

For sale by the Clearinghouse for Federal Scientific and Technical Information
Springfield, Virginia 22151 – CFSTI price $3.00

COMPUTER SIMULATION OF A CYLINDRICAL GALAXY

By Frank Hohl
Langley Research Center

SUMMARY

A two-dimensional computer model is used to investigate the evolution of a self-gravitating cylindrical galaxy. The evolution of systems containing up to 100 000 mass rods is investigated by following the self-consistent motion of the mass rods. As the system evolves in time, it displays the various shapes observed in actual galaxies; however, any spiral structure which appears during the initial stages of the evolution disappears after about 10 rotations, and the final state of the system is that of a rotating bar or a circular cluster with a high central condensation. It is found that violent relaxation or phase mixing causes any unstable system quickly to build up large random velocities. The rate of buildup of random motions in stable systems was found to be described by a Chandrasekhar-type relaxation time.

INTRODUCTION

Two-dimensional computer models have recently been used by Hockney (ref. 1) and by Hohl (refs. 2 to 4) to simulate the evolution of collisionless self-gravitating systems. In the two-dimensional model, the N stars in the system are represented by infinitely long mass rods which have a mass m per unit length. These stars are then allowed to move in the two directions perpendicular to their axes. This approximation leads to a completely two-dimensional problem and greatly simplifies the calculation of the gravitational potential.

In the present calculations the number of stars in the system has been greatly increased as compared to the calculations previously made (ref. 4). The results indicated that especially for systems containing small numbers of stars, the detailed structure displayed by a system depended markedly on the number of stars in the system. Also, the systems quickly build up temperature or random motion of the stars which destroys any spiral structure. Tests were performed to determine whether the randomization was caused by collisional effects introduced by the model or by the violent relaxation proposed by Lynden-Bell (ref. 5) and investigated by Hohl and Campbell (ref. 6).

SYMBOLS

a	major axis; also, acceleration
b	minor axis
D	distance
g	gravitational field
G	gravitational constant
m	mass per unit length
M	total mass per unit length
n	star density
N	total number of stars
P	potential energy
r	radius, $\sqrt{x^2 + y^2}$
t	time
T	kinetic energy
U	total energy, $T + P$
V	velocity
V_g	rms value of relative velocity in balanced cylinder
V_T	transverse velocity
x,y	positions along x and y axes, respectively
z	complex coordinate, $x + iy$

γ	convergence parameter
ρ	mass density
τ_c	relaxation time
τ_g	equilibrium rotation period
φ	gravitational potential
ω	frequency of rotation
ω_g	equilibrium frequency of rotation

Subscripts:

i,j,k,n,m	summation indices
max	maximum
min	minimum
r	radial
x,y	x- and y-component
θ	azimuthal
$\langle\ \rangle$	denotes expectation values

MODEL AND METHOD OF SOLUTION

The model consists of a large number of mass rods. The position and velocity of all the mass rods is stored in the computer. Newton's laws of motion and Newton's theory of gravitation are used to advance the position and velocity of all the stars stepwise in time.

The area which contains the galaxy of stars is divided into a square array of cells (usually 101×101). At the center of each cell a mass density $\rho_{n,m}$ is defined which is given by the number of stars in that cell. The integers n and m increase in the

x- and y-direction, respectively. The gravitational potential $\varphi_{n,m}$ is then obtained from the density $\rho_{n,m}$ by solving the two-dimensional Poisson equation

$$\frac{\partial^2 \varphi}{\partial x^2} + \frac{\partial^2 \varphi}{\partial y^2} = 4\pi G\rho(x,y) \tag{1}$$

by finite difference methods (ref. 4). The standard five-point difference equation (ref. 7)

$$\varphi_{n+1,m} + \varphi_{n,m+1} + \varphi_{n-1,m} + \varphi_{n,m-1} - 4\varphi_{n,m} = 4\pi G\rho_{n,m} \tag{2}$$

was used to solve for the potential distribution. The cell dimensions Δx and Δy are taken to be equal to unity. This set of simultaneous equations is solved by an iteration method on the Control Data 6600 computer in the form

$$\varphi^{r+1}_{n,m} = \varphi^{r}_{n,m} + \gamma\left(\varphi^{r+1}_{n-1,m} + \varphi^{r}_{n+1,m} + \varphi^{r+1}_{n,m-1} + \varphi^{r}_{n,m+1} - 4\varphi^{r}_{n,m} - 4\pi G\rho_{n,m}\right) \tag{3}$$

For the purpose of saving computer storage and increasing the convergence rate, the new values of φ (that is, φ^{r+1}) which have already been calculated during a particular iteration are used in the right-hand side of equation (3). The superscript r refers to the rth iteration and the parameter γ is adjusted to give the maximum rate of convergence. The potential at the boundary of the rectangular region is required in the solution of the Poisson equation. At an arbitrary boundary point a distance $z = x + iy$ from the center of the mesh, the potential is given by

$$\varphi(z) = 2G \sum_{n,m} \rho_{n,m} \log_e|z - z_{n,m}| = 2GM \log_e|z| + 2G \sum_{n,m} \rho_{n,m}\, \mathrm{Re}\left[\log_e\left(1 - \frac{z_{n,m}}{z}\right)\right] \tag{4}$$

where M is the total mass in the system and $z_{n,m} = x_{n,m} + iy_{n,m}$ is the coordinate of the cell n,m. Since $\rho_{n,m}$ is nonzero only for $\left|\frac{z_{n,m}}{z}\right| < 1$, equation (4) can be written as

$$\varphi(z) = 2GM \log_e|z| - 2G\,\mathrm{Re} \sum_{k} \frac{a_k}{k z^k} \tag{5}$$

where

$$a_k = \sum_{n,m} \rho_{n,m} z^k_{n,m} \tag{6}$$

and the series expansion for $\log_e\left(1 - \frac{z_{n,m}}{z}\right)$ has been truncated after 15 terms.

If the motion of all the stars in the system is advanced for a small time step δt, the mass distribution $\rho_{n,m}$ will not change very much. The change in the gravitational potential will then also be very small. Thus, the solution of the finite difference form of the Poisson equation (eq. (3)) by an iteration method which uses the potential from the previous cycle as an initial guess will converge very rapidly. The accuracy of the iterative solution of the Poisson equation is continually checked during the calculations. This verification is made by obtaining the values of the potential and the field at several selected points by summing directly the contribution from each star. The values so obtained agree with those obtained from the solution of the Poisson equation to at least the first three digits. The number of iterations required for a 51×51 mesh was 5 to 7 and for a 101×101 mesh, 12 iterations. The calculation time for one cycle of a 10 000-star system with a 101×101 mesh is 7 seconds on the Control Data 6600 computer. This time includes such operations as checking of the gravitational potential, calculation of the energy and angular momentum, and writing the positions and velocities of all stars on tape.

The initial guess of the potential at $t = 0$ was determined by using the analytical expression for the potential of a homogeneous elliptical cylinder. (See ref. 8.) If the cylinder containing N stars of unit mass is described by

$$\frac{x^2}{a^2} + \frac{y^2}{b^2} = 1$$

the potential interior to this cylinder is given by

$$\varphi(x,y) = \frac{2NG}{a+b}\left(\frac{x^2}{a} + \frac{y^2}{b}\right) + \varphi(0,0)$$

where

$$\varphi(0,0) = 2G \sum_{n,m} \rho_{n,m} \log_e \left| z_{n,m} \right|$$

and $z_{n,m}$ is the position of a cell measured from the center of the mesh. For points exterior to the cylinder, the potential is

$$\varphi(x,y) = 2GN\left[\frac{x^2}{a^2 + \kappa + \sqrt{(b^2+\kappa)(a^2+\kappa)}} + \frac{y^2}{b^2 + \kappa + \sqrt{(b^2+\kappa)(a^2+\kappa)}}\right]$$

where

$$\kappa = \frac{1}{2}\left[x^2 + y^2 - a^2 - b^2 + \sqrt{\left(a^2 + b^2 - x^2 - y^2\right) - 4\left(a^2b^2 - b^2x^2 - a^2y^2\right)}\right]$$

The motion of the stars is described by the differential equations

$$\left.\begin{aligned} \frac{dV_x}{dt} &= -\frac{\partial \varphi}{\partial x} \\ \frac{dV_y}{dt} &= -\frac{\partial \varphi}{\partial y} \end{aligned}\right\} \tag{7}$$

and

$$\left.\begin{aligned} V_x &= \frac{dx}{dt} \\ V_y &= \frac{dy}{dt} \end{aligned}\right\} \tag{8}$$

For a star in the (n,m)th cell equations (7) and (8) are in finite difference form

$$\frac{1}{\delta t}\left[V_x\left(t + \frac{\delta t}{2}\right) - V_x\left(t - \frac{\delta t}{2}\right)\right] = \frac{1}{2}\left(\varphi_{n-1,m} - \varphi_{n+1,m}\right) \tag{9}$$

and

$$\frac{1}{\delta t}\left[x(t + \delta t) - x(t)\right] = V_x\left(t + \frac{\delta t}{2}\right) \tag{10}$$

with similar equations for the y-components. As given by equation (9), all stars in the cell n,m experience the same gravitational field. For the calculations reported in the present paper, the field acting on a star was obtained by means of a bilinear interpolation of the fields at the four cell centers surrounding the position of the particle. The right-hand side of equation (9) is then replaced by the interpolated field. The new velocity $V\left(t + \frac{\delta t}{2}\right)$ and position $x(t + \delta t)$ are then obtained from those at the beginning of the time step by means of the equations

$$\begin{aligned} V_x\left(t + \frac{\delta t}{2}\right) = V_x\left(t - \frac{\delta t}{2}\right) + \frac{\delta t}{2}\Big[&(1 + \delta y)(1 - \delta x)\left(\varphi_{n+1,m} - \varphi_{n-1,m}\right) \\ &+ \delta y(1 - \delta x)\left(\varphi_{n+1,m+1} - \varphi_{n-1,m+1}\right) + \delta x(1 - \delta y)\left(\varphi_{n+2,m} - \varphi_{n,m}\right) \\ &+ \delta x\, \delta y\left(\varphi_{n+2,m+1} + \varphi_{n,m+1}\right)\Big] \end{aligned} \tag{11}$$

and

$$x(t + \delta t) = x(t) + \delta t V_x\left(t + \frac{\delta t}{2}\right) \tag{12}$$

One complete cycle for advancing the motion of the system by a time δt consists of the following steps. First, the distribution of mass $\rho_{n,m}$ is used to obtain the gravitational potential $\varphi_{n,m}$ by numerically solving the Poisson equation. Second, the gravitational field at the position of the stars is computed from the potential $\varphi_{n,m}$. Third, Newton's laws of motion are used to advance the motion of all the mass rods for a small time step δt. These three steps represent one cycle and are repeated until the desired evolution of the system is achieved.

The kinetic energy of the system at time t is

$$T = \frac{1}{2}\sum_{j=1}^{N} m_j \left\{ \left[\frac{V_x\left(t + \frac{\delta t}{2}\right) + V_x\left(t - \frac{\delta t}{2}\right)}{2} \right]^2 + \left[\frac{V_y\left(t + \frac{\delta t}{2}\right) + V_y\left(t - \frac{\delta t}{2}\right)}{2} \right]^2 \right\} \tag{13}$$

where the summation extends over all stars and the potential energy is

$$P = \frac{1}{2}\sum_{n,m} \rho_{n,m}\varphi_{n,m} \tag{14}$$

The total energy U of the system is given by

$$U = T + P \tag{15}$$

For most of the systems investigated the calculated total energy during a given computer run was conserved to within 0.5 percent and the angular momentum remained practically constant.

RESULTS AND DISCUSSION

Computer simulations have been performed for a number of systems with an initially uniform distribution over a circular or elliptical region in x,y-coordinate space, zero thermal velocity, and various values of initial solid-body rotation. In particular, systems with a ratio of major axis a to minor axis b of 3 and with an initial solid-body rotation given by

$$\omega^2 = \omega_g{}^2 = \frac{8MG}{(a + b)^2} \tag{16}$$

have been investigated in detail. The ω_g given by equation (16) will initially approximately balance the gravitational attraction. It was found that for a system containing 2000 stars with a 51×51 grid to solve the Poisson equation, randomization effects destroyed the spiral structure after only 2 to 3 rotations. The results are shown in figures 1 to 3. The normalization $G = m = 1$ was used in the calculations and the time

is shown in rotation periods $\tau_g = \frac{2\pi}{\omega_g}$. Figure 1 shows the evolution of the 2000-star system in x,y-coordinate space. These results show that any structure which appears initially quickly randomizes after less than 3 rotations. The evolution of the velocity distribution in V_x, V_y-space is shown in figure 2. Figure 3 shows the evolution of the velocity distribution in coordinates that rotate with the equilibrium angular velocity ω_g. The velocity $(V_\theta - r\omega_g)$ where V_θ is the azimuthal velocity and r is the radius from the center of the system to a star is plotted as a function of the radial velocity V_r. The velocities in figures 2 and 3 are plotted on nearly equal scales. Initially, the thermal (or random) velocity of all mass rods is zero since initially the system has a solid-body rotation only. As the system evolves in time the thermal velocity builds up quickly and the system expands in $(V_\theta - r\omega_g), V_r$-space. After a time $t = 1.75\tau_g$ the random velocities are of the same order as the initial circular velocities and there is little further change in the velocity distribution. The long tail in the velocity distribution in figure 3 is due to differential rotation. These results indicate that for the calculations reported by Hockney (ref. 1) with 2000 stars and a 48×48 grid, the system randomizes in about 2 rotations. The same holds for the results given by Hohl (refs. 3 and 4) for 2000 stars (with a 51×51 grid). To reduce the randomization effects (i.e., fluctuations of order $1/\sqrt{N}$) the calculations were repeated with an identical initial elliptical distribution but with 4000 stars and a 101×101 grid to solve the Poisson equation. The results are shown in figures 4 and 5. Figure 4 shows that the spiral structure now has a somewhat greater stability but still tends to randomize after about 4 rotations. The corresponding evolution in V_x, V_y-velocity space is shown in figure 5. The calculations were repeated with the number of stars increased to 10 000; the resulting evolution in x,y-coordinate space is shown in figure 6. Figure 6(b) shows that at $t = 6\tau_g$ the spiral structure begins to randomize. From these results it appears that in order to simulate collisionless systems for the first n rotations, nearly $2n \times 10^3$ stars are required.

An interesting point is that all systems investigated which have an initially elongated distribution and a given solid-body rotation go through an initial evolution similar to that shown in figure 6(a) up to $t = 1.0\tau_g$. At $t = 0.75\tau_g$ the system shows a structure nearly identical to that of the peculiar galaxy (GB 1) discussed by Burbidge, Burbidge, and Shelton (ref. 9). Another such integral-sign-shaped galaxy is NGC 4656/7 reproduced in the Hubble Atlas (ref. 10, p. 40). Figure 6 shows that at $t = 3.0\tau_g$ the two spiral arms begin to overlap and give the appearance of a circular ring of stars separate from the nucleus, presenting a shape similar to NGC 3145 (ref. 10, p. 21). At $t = 4.0\tau_g$ the system shows a structure similar to NGC 5194 (ref. 10, p. 31). Furthermore, at $t = 3.0\tau_g$ the spiral structure has almost disappeared and at $t = 3.75\tau_g$, after less than one rotation, the spiral structure is again very pronounced. This phenomenon appears to reoccur from $t = 4.50\tau_g$ to $t = 6.00\tau_g$. However, at $t = 6.00\tau_g$ randomization

effects have already appreciably affected the evolution of the system. This behavior indicates that the spiral arms may be short lived but re-form repeatedly as in the theory of Goldreich and Lynden-Bell (ref. 11). Since the spiral arms do not remain for a long time it is difficult to determine whether the stars that are in a particular arm remain there, as in the theory of Goldreich and Lynden-Bell, or whether they move from arm to arm as would be expected from the theory of Lin and Shu (refs. 12 and 13). The evolution of the velocity distribution for the 10 000-star system is shown in figure 7. At $t = 0.25\tau_g$ the system shows an interesting structure. Condensation in velocity space has occurred and striation appears in the velocity distribution. The corresponding evolution in $\left(V_\theta - r\omega_g\right), V_r$-velocity space is shown in figure 8. This distribution shows little change after the first 3 rotations. Again, the scales for plotting the velocity distributions in figures 7 and 8 are about the same.

The number of stars in the system was finally increased to 100 000 to determine whether a more stable spiral structure would result. The evolution in x,y-coordinate space for the 100 000-star system is shown in figure 9. These results show that no stable spiral structure develops even for large numbers of stars in the system.

The effect of giving the system an initial rotation 30 percent larger than that given by equation (16) is shown in figure 10. There are 10 000 stars in the system. Figure 10 shows that the initially increased speed of rotation causes the system to break up into clusters and evolve more irregularly as compared with the system shown in figure 6. After 15 rotations the system has a bar shape with a diffuse cloud of stars around the bar. The long-time evolution of various systems investigated shows that the bar shape structure is favored as the final state of the system.

The effect of placing a large mass at the center of the system was also investigated. Figure 11 shows the positions of the 10 000 stars in the system at different times. The central mass has 10 times the mass of the 10 000 stars in the system. The initial distribution was chosen to produce a spiral structure. The time is given in arbitrary units. The figure shows that the spiral pattern simply winds up because of differential rotation. No persistent spiral pattern is found.

The evolution and the final state of a system might be expected to depend on the initially elongated distribution. The evolution of systems with initially circular distributions in coordinate space were therefore investigated. Figure 12 shows the evolution of a 10 000-star system with an initially uniform distribution over a circular region and with an initial solid-body rotation equal to that required to balance gravitation. The gravitational field g inside such a system is

$$g = 2\pi G\rho r \tag{17}$$

To balance this gravitational field requires a centrifugal force equal to $\omega^2 r$ where

$$\omega = \sqrt{2\pi G\rho} \tag{18}$$

The rotational period for such a system is therefore

$$\tau_g = \frac{2\pi}{\sqrt{2\pi G\rho}} \tag{19}$$

Figure 12 shows that for the first 2 rotations the evolution of the balanced cylinder containing 10 000 stars is very similar to that of the 2000-star system investigated by Hockney (ref. 1) and by Hohl and Park (ref. 4). For these 2000-star systems of references 1 and 4, the results showed that the relatively small fourth-mode surface wave around the periphery of the cylinder quickly changed to a second-mode surface wave (egg shape), then all structure was lost, and the system finally assumed a circular shape. This sequence is due to the large randomizations (pressure) that developed to balance the gravitational attraction towards the center of the system. Figure 12 shows that the evolution is quite different when randomization effects are reduced by increasing the number of particles to 10 000. The fourth-mode surface wave now continues to grow and after 5 rotations a four-arm spiral begins to form. After about 8 rotations two of the arms have disappeared and the system has assumed a bar shape. Figures 13 and 14 are plotted on the same scale and they show that after about 9 rotations the random or thermal velocities have increased to such an extent that they are of the same magnitude as the rotational velocities. The evolution of random velocities shown in figure 14 shows an almost linear increase in the random or thermal motion of the mass rods. Figure 12 shows that the second-mode surface wave will finally dominate and the system assumes a bar shape which appears to be the most probable state for the system. Figure 15 shows, again, the evolution of a 10 000-star system like that shown in figure 12. The only difference is that a different pseudo-random number sequence was used for the initial positions of the stars. The evolution is very similar to that shown in figure 12 and again the final state is a bar-shape system. When the trajectories of individual stars are plotted they are found to oscillate in the potential well set up by the high mass concentration in the bar.

It is of interest to determine the extent to which randomization or collisional effects are present in the computer model. The relaxation time τ_c (ref. 14) can be approximated by applying the method for point stars (ref. 15) to mass rods.

Consider an encounter between a rod of mass m_2 and velocity V with a stationary rod of mass m_1. If D is the distance of closest approach (impact parameter) then the transverse force acting on the moving star m_2 during a time $2D/V$ can be approximated as $2Gm_1m_2/D$. The moving star has therefore acquired a transverse velocity

$$\delta V_T \cong \frac{4Gm_1}{V} \tag{20}$$

For a star interacting with a system containing many stars, the effect of many individual encounters must be summed. The number of encounters in a time t with impact parameter between D and $D + dD$ is $tVn\,dD$ where n is the density of stars in the system. The expectation value of V_T^2 is then given by

$$\left\langle V_T^2 \right\rangle = \int_{D_{min}}^{D_{max}} \frac{16tnG^2m_1^2}{V}\,dD = \frac{16tnG^2m_1^2(D_{max} - D_{min})}{V} = \frac{16tnG^2m_1^2D_{max}}{V} \tag{21}$$

since in general $D_{max} >> D_{min}$ where D_{max} is the dimension of the system and D_{min} is the cell size used in the calculations. The relaxation time τ_c is defined to be the time required for $\left\langle V_T^2 \right\rangle$ to be of the same order of magnitude as V^2. Equation (21) then becomes

$$\tau_c = \frac{V_g^3}{16\rho mG^2D_{max}} \tag{22}$$

where V_g is the root-mean-square value of the velocity of the stars and D_{max} is the radius of the system. Consider now a uniformly rotating cylinder of stars of radius D_{max} and constant density ρ. The period of rotation is given by equation (19) and the mean quadratic difference of velocity between two stars is

$$V_g = D_{max}(2\pi G\rho)^{1/2} \tag{23}$$

The ratio of the relaxation time τ_c to the rotational period τ_g is then

$$\frac{\tau_c}{\tau_g} = \frac{\pi D_{max}^2 n}{8} = \frac{N}{8} \tag{24}$$

Equation (24) is a rough estimate but it indicates that for a system containing 10 000 stars, randomization effects would be expected to occur after about 1000 rotations. Since the observed randomization for the unstable system occurs after only a few rotations, the Chandrasekhar-type (ref. 14) calculation (eq. (22)) of the relaxation time does not apply. For a system with an initial solid-body rotation there is only one velocity at any given point. Thus, in the neighborhood of any particular star very little relative motion is present and the usual assumption of random motions underlying the calculation of the relaxation time does not apply. It was suggested by Dr. M. Hénon of Observatoire de Nice (France) in a personal communication to the author that the following estimate of the relaxation time may be more appropriate. The acceleration at a distance D away from a single star is $2Gm/D$. At the center of the system the expectation value of the square of the total acceleration a is therefore

$$\left\langle a^2 \right\rangle = \int_{D_{min}}^{D_{max}} \frac{4G^2m^2}{D^2} 2\pi nD \, dD = 8\pi\rho G^2 m \log_e \frac{D_{max}}{D_{min}} \tag{25}$$

If the acceleration is taken to be constant, the perturbations in the velocity of the stars $\left\langle V_T^2 \right\rangle$ will grow as the square of the time

$$\left\langle V_T^2 \right\rangle = t^2 \left\langle a^2 \right\rangle$$

This result is in agreement with the results shown in figure 14. In the usual case $\left\langle V_T^2 \right\rangle$ grows linearly with time. The relaxation time τ_c is defined to be the time required for $\left\langle V_T^2 \right\rangle$ to be of the same order of magnitude as V_g^2. Thus,

$$\tau_c = \sqrt{\frac{\left\langle V_g^2 \right\rangle}{\left\langle a^2 \right\rangle}}$$

and

$$\frac{\tau_c}{\tau_g} = \frac{1}{4\pi} \left(\frac{N}{\log_e \frac{D_{max}}{D_{min}}} \right)^{1/2} \tag{26}$$

The distance D_{min} is equal to the dimension of a cell so that $\frac{D_{max}}{D_{min}} \approx 51$ and

$$\frac{\tau_c}{\tau_g} = \frac{\sqrt{N}}{25} \tag{27}$$

For $N = 2000$, 4000, and 10 000 the corresponding values of τ_c/τ_g are 1.8, 2.5, and 4.0, which are in good agreement with the numerical results. This type of fast relaxation which occurs in unstable systems is the violent relaxation or phase mixing described by Lynden-Bell (ref. 5).

The results given in figures 12 and 15 show that the uniformly rotating cylinder is unstable. Figure 16 shows the effect on the stability when one-half of the stars rotate clockwise and the other half rotate counterclockwise. The cylinder is now stable and retains its original shape even after many rotations. Figure 17 shows the variation of the total kinetic energy for the stable cylinder shown in figure 16. The initial small oscillations are quickly damped out. The variation of the kinetic energy for the unstable systems shown in figures 12 and 15 is essentially identical to that shown in figure 17. Because the system of counterrotating stars is stable, it is suited for determining the rate at which thermalization effects occur in the two-dimensional model. These effects are calculated by determining the rate at which equipartition of energy occurs among stars of different masses. Initially, the balanced system contains a uniform distribution

of 5000 stars of mass $m_1 = \frac{3}{2} m$ rotating clockwise plus a uniform distribution of 5000 stars of mass $m_2 = \frac{1}{2} m$ rotating counterclockwise. The resulting evolution of the system is shown in figures 18 and 19. The normalized kinetic energy for the heavy stars is now defined as

$$T_1^* = \frac{T_1}{m_1} = \frac{1}{2} \sum_i V_i^2 \qquad \text{(heavy stars)}$$

where the summation extends over the 5000 heavy stars. Similarly for the light stars

$$T_2^* = \frac{T_2}{m_2} = \frac{1}{2} \sum_j V_j^2 \qquad \text{(light stars)}$$

Figure 20 shows the percent variation of the difference between T_1^* and T_2^*. Initially, the heavy stars have an excess of kinetic energy because of their larger mass. The total unnormalized kinetic energy of the heavy stars is $\frac{3}{2} mT_1^*$ and the unnormalized kinetic energy of the light stars is $\frac{1}{2} mT_2^*$. The fast drop in the energy T_1^* during the first 2 rotations is probably due to collective effects, as are the oscillations shown after 4 rotations. However, figure 20 clearly shows that the heavy stars are losing kinetic energy, and after 11 rotations the average value of T_2^* is 0.5 percent of the total kinetic energy larger than T_1^*. For equipartition of energy between the heavy and the light stars, $T_2^* = 3T_1^*$. If the same rate of increase in T_2^* as shown in figure 20 is assumed, then equipartition would be achieved after about 1100 rotations, which is in good agreement with the value 1250 given by equation (24) for $N = 10\,000$.

CONCLUDING REMARKS

The results obtained with the two-dimensional model for a self-gravitating cylindrical galaxy show that as the system evolves in time, it displays the various shapes observed in actual galaxies. However, the rod-star approximation is likely to be valid only for very few galaxies, such as the cigar-shaped galaxy NGC 2685. In order to simulate the evolution of systems like spiral galaxies, calculations are now in progress for systems consisting of finite length mass rods and point masses moving in a plane.

It was found that for stable systems the Chandrasekhar-type calculation of the relaxation time was applicable and that the stable two-dimensional model can indeed be

considered collisionless. The fast randomization which occurred for unstable systems must be ascribed to violent relaxation or phase mixing as predicted by Lynden-Bell.

Langley Research Center,
National Aeronautics and Space Administration,
Langley Station, Hampton, Va., March 3, 1969,
129-02-01-01-23.

REFERENCES

1. Hockney, R. W.: Gravitational Experiments With a Cylindrical Galaxy. Astrophys. J., vol. 150, no. 3, Dec. 1967, pp. 797-806.

2. Hohl, Frank: One- and Two-Dimensional Models to Study the Evolution of Stellar Systems. Symposium on Computer Simulation of Plasma and Many-Body Problems. NASA SP-153, 1967, pp. 323-336.

3. Hohl, Frank: Computer Solutions of the Gravitational N-Body Problem. Extrait Bull. Astron., Ser. 3, Tome III, Fasc. 2, 1968, pp. 227-240.

4. Hohl, Frank; and Park, Stephen K.: Gravitational Experiments With a Collisionless Two-Dimensional Computer Model. NASA TN D-4646, 1968.

5. Lynden-Bell, D.: Statistical Mechanics of Violent Relaxation in Stellar Systems, Mon. Notic. Roy. Astron. Soc., vol. 136, no. 1, 1967, pp. 101-121.

6. Hohl, Frank; and Campbell, Janet W.: Statistical Mechanics of a Collisionless Self-Gravitating System. Astron. J., vol. 73, no. 7, Sept. 1968, pp. 611-615.

7. Forsythe, George E.; and Wasow, Wolfgang R.: Finite-Difference Methods for Partial Differential Equations. John Wiley & Sons, Inc., c.1960.

8. MacMillan, William Duncan: The Theory of the Potential. McGraw-Hill Book Co., Inc., 1930, pp. 69-72.

9. Burbidge, E. Margaret; Burbidge, G. R.; and Shelton, J. W.: A Peculiar Galaxy That May Be at a Young Evolutionary Stage. Astrophys. J., vol. 150, no. 3, Dec. 1967, pp. 783-786.

10. Sandage, Allan: The Hubble Atlas of Galaxies. Publi. 618, Carnegie Institution of Washington (Washington, D.C.), 1961.

11. Goldreich, P.; and Lynden-Bell, D.: II. Spiral Arms as Sheared Gravitational Instabilities. Mon. Notic. Roy. Astron. Soc., vol. 130, nos. 2 & 3, 1965, 125-158.

12. Lin, C. C.; and Shu, Frank H.: On the Spiral Structure of Disk Galaxies. Astrophys. J., vol. 140, no. 2, Aug. 1964, pp. 646-655.

13. Lin, C. C.; and Shu, Frank H.: On the Spiral Structure of Disk Galaxies, II. Outline of a Theory of Density Waves. Proc. Nat. Acad. Sci., vol. 55, no. 2, Feb. 1966, pp. 229-234.

14. Chandrasekhar, S.: Principles of Stellar Dynamics. Enlarged ed., Dover Publ., Inc., 1960.

15. Woltjer, L.: Structure and Dynamics of Galaxies. Relativity Theory and Astrophysics – 2. Galactic Structure, Jürgen Ehlers, ed., Amer. Math. Soc., 1967, pp. 1-65.

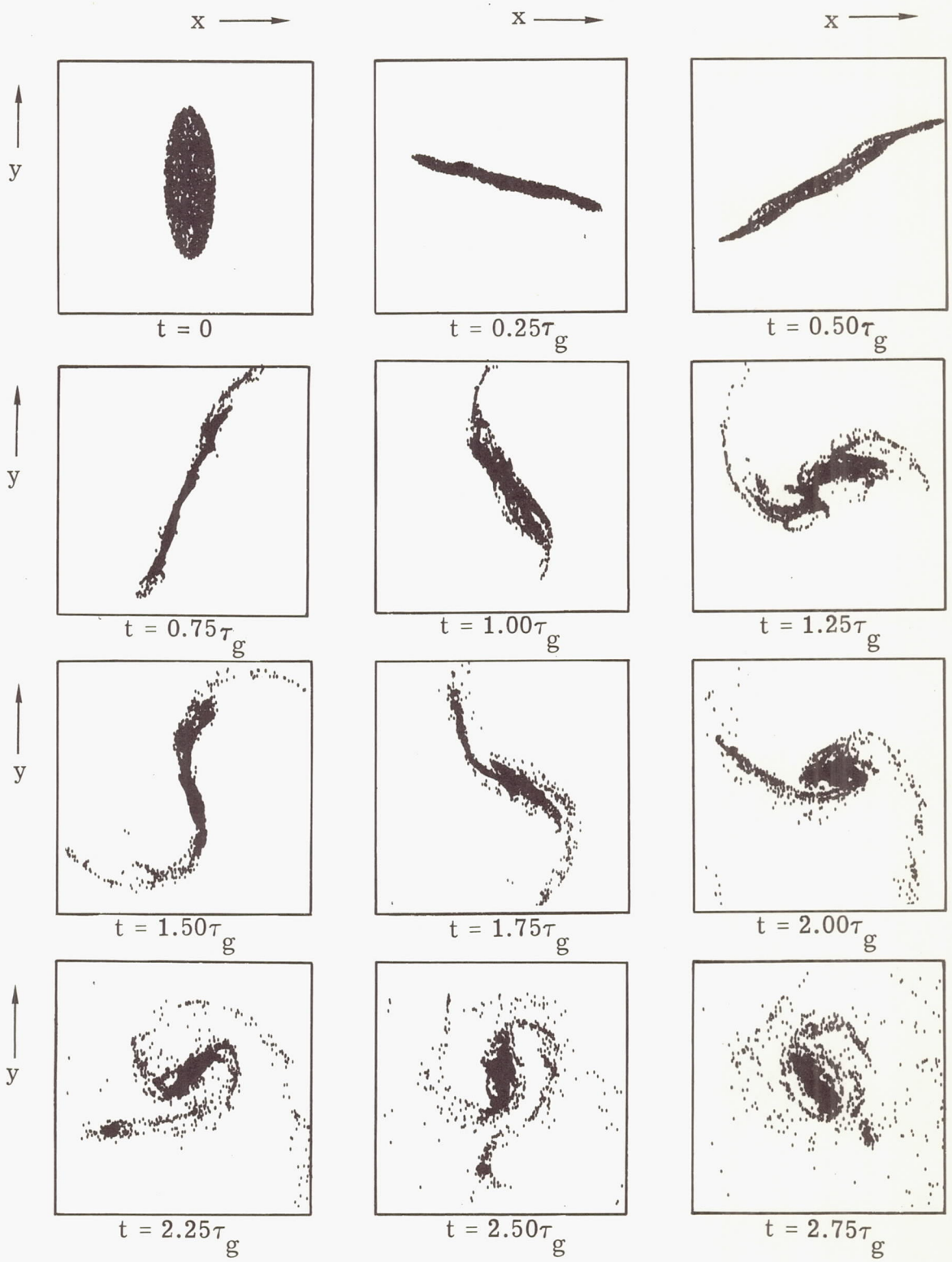

Figure 1.- Evolution of a 2000-star system in coordinate space.

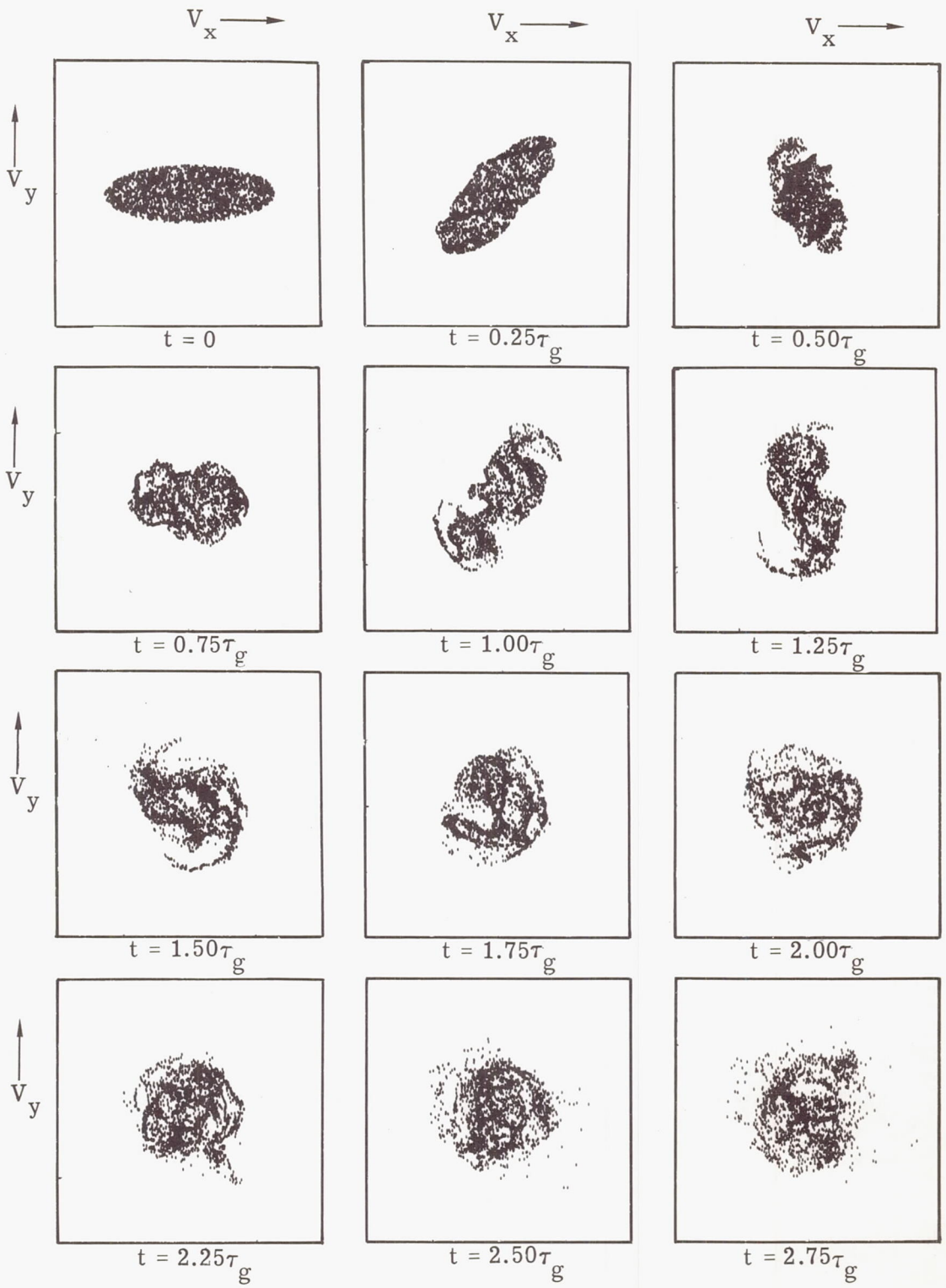

Figure 2.- Evolution of a 2000-star system in V_x,V_y-velocity space.

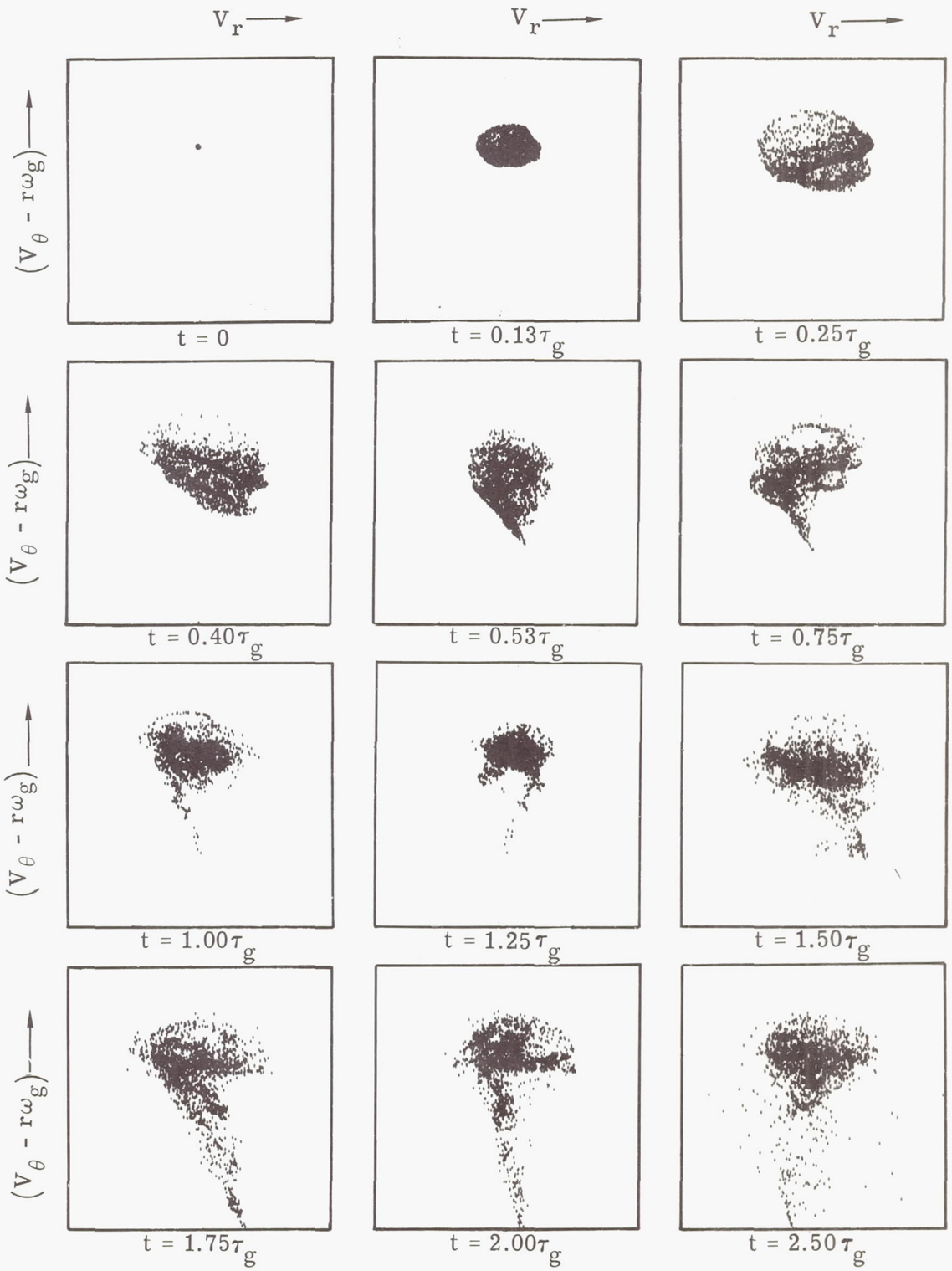

Figure 3.- Evolution of a 2000-star system in $(V_\theta - r\omega_g)$,V_r-velocity space.

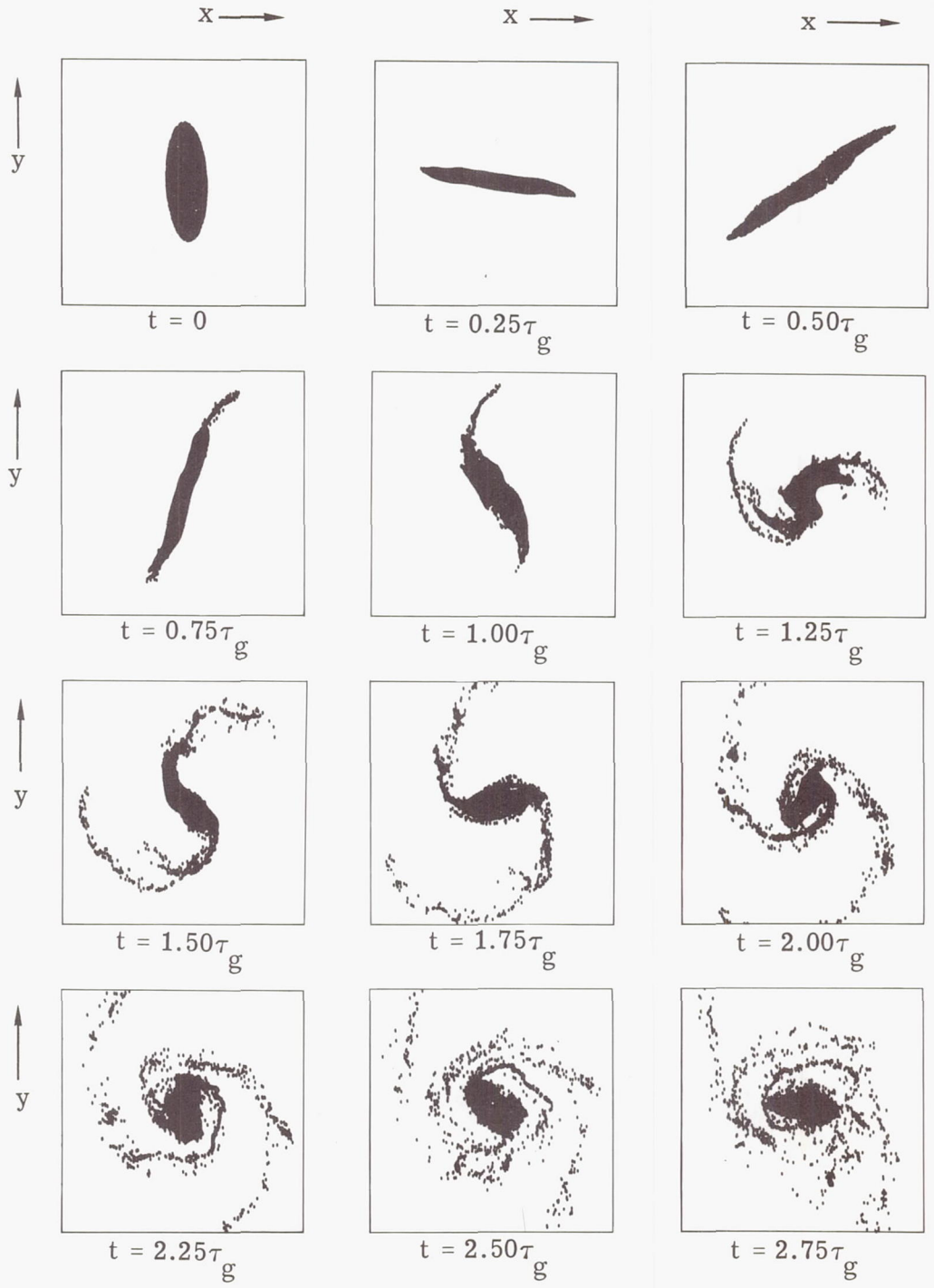

(a) Evolution up to $t = 2.75\tau_g$.

Figure 4.- Evolution of a 4000-star system in x,y-coordinate space.

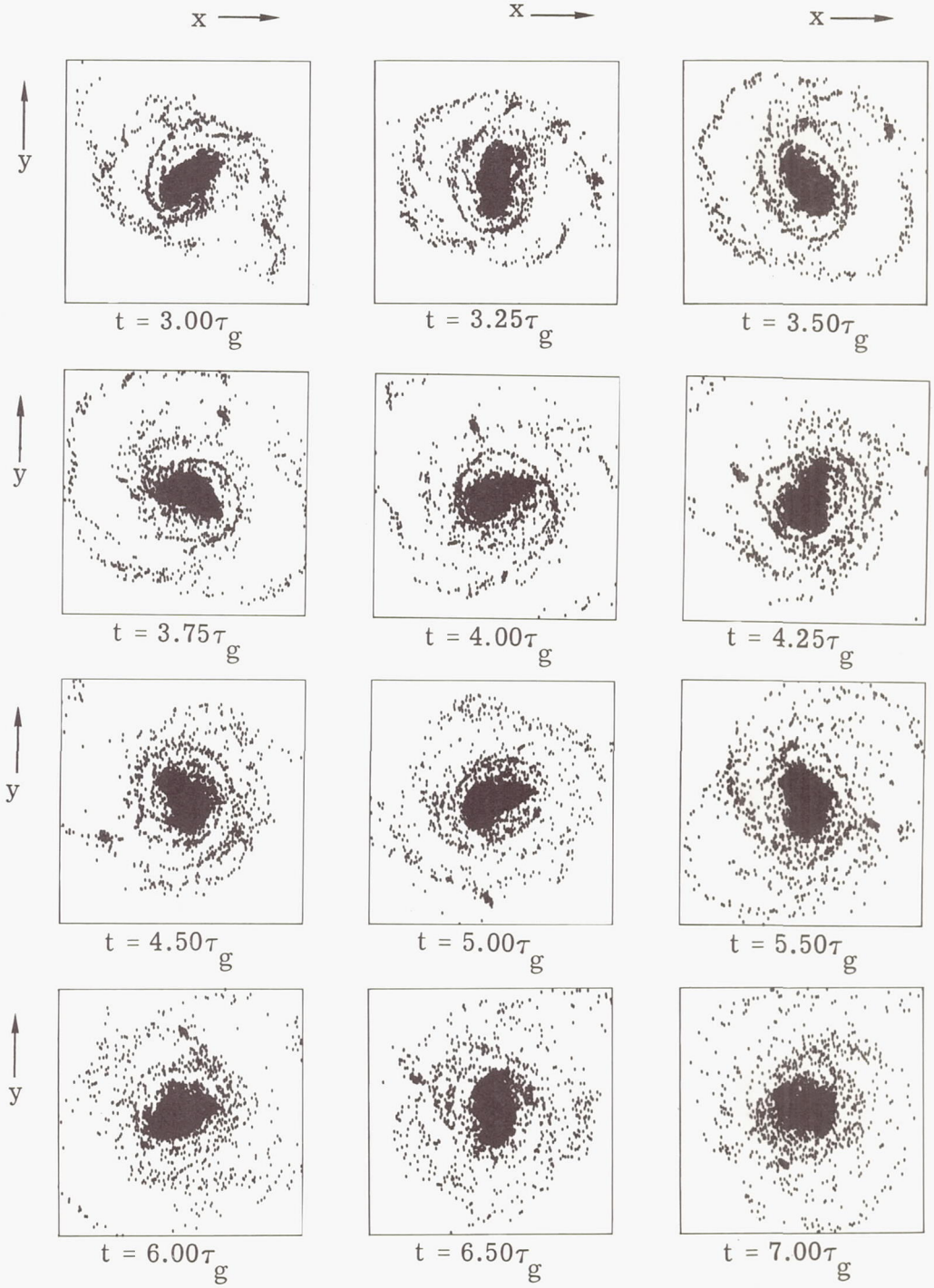

(b) Evolution up to $t = 7.00\tau_g$.

Figure 4.- Concluded.

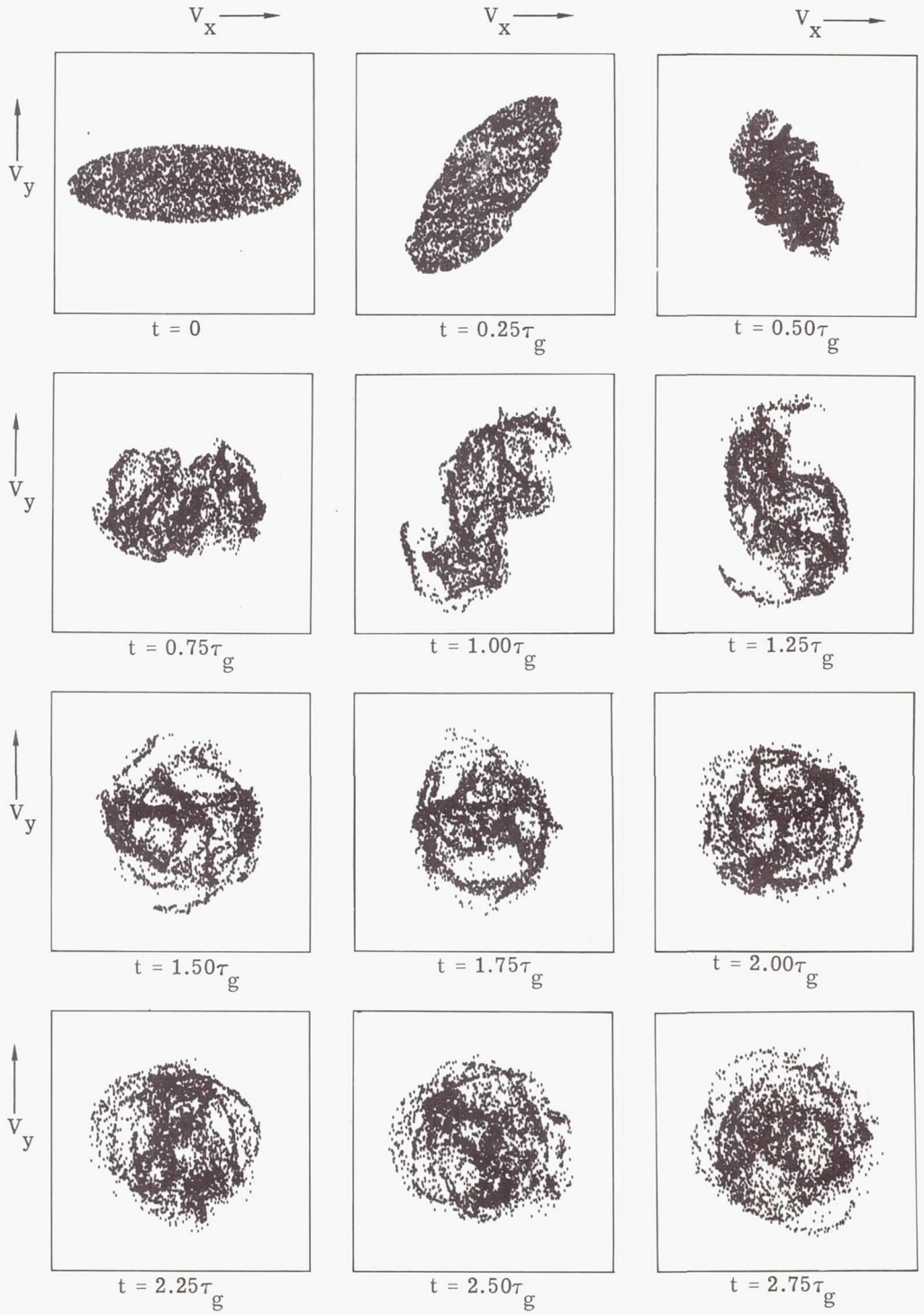

(a) Evolution up to $t = 2.75\tau_g$.

Figure 5.- Evolution of a 4000-star system in V_x,V_y-velocity space.

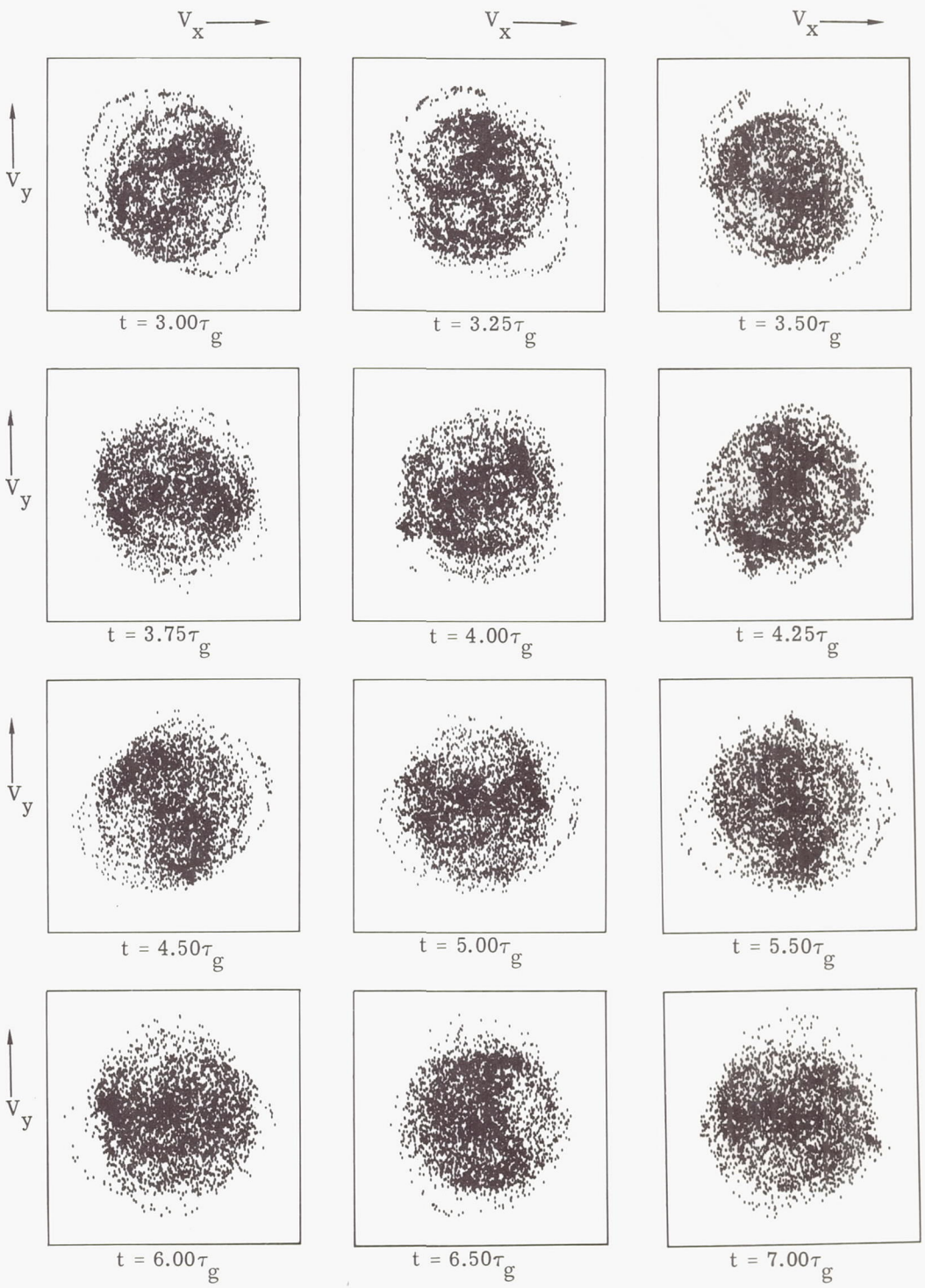

(b) Evolution up to $t = 7.00\tau_g$.

Figure 5.- Concluded.

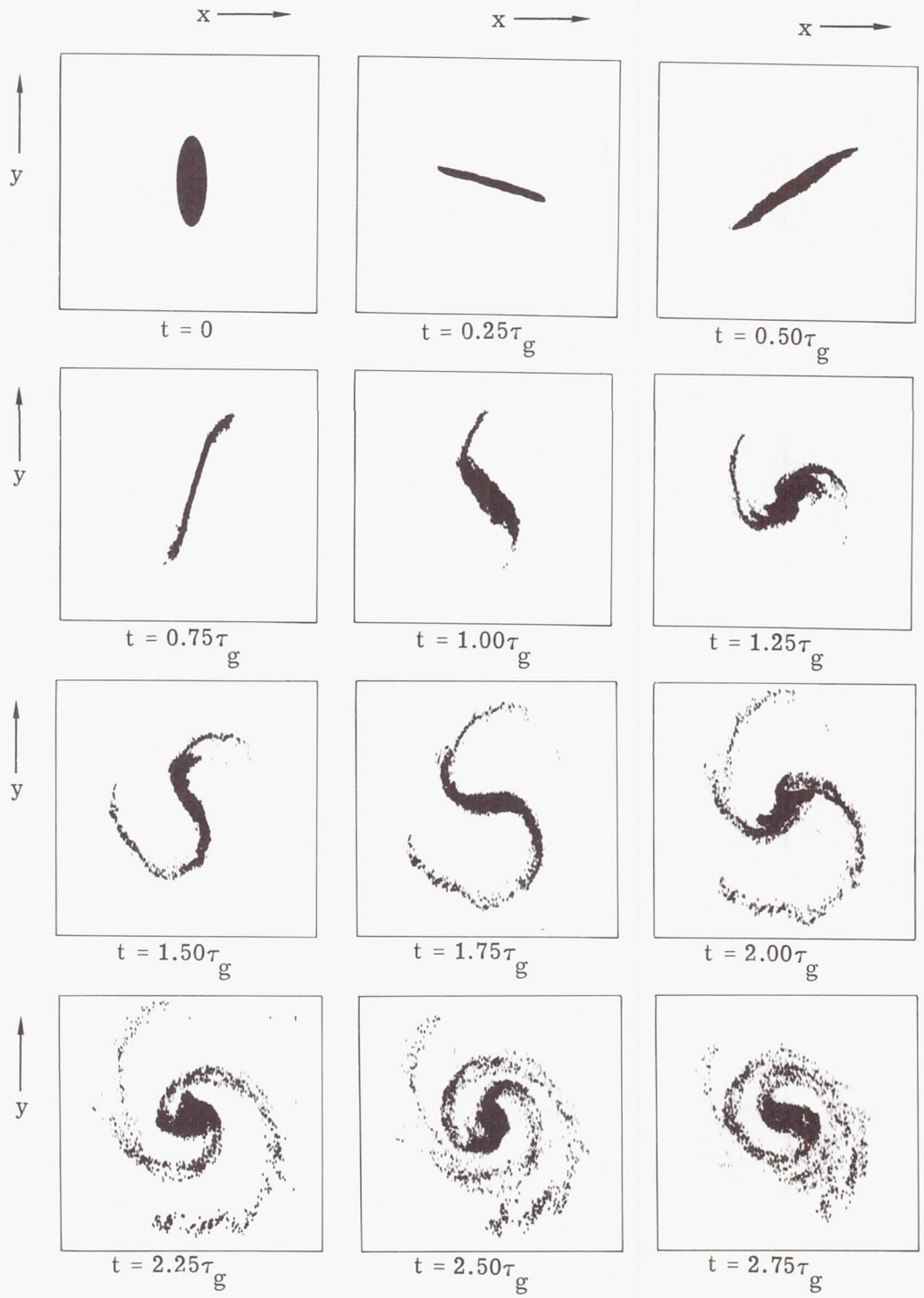

(a) Evolution up to $t = 2.75\tau_g$.

Figure 6.- Evolution of a 10 000-star system in x,y-coordinate space.

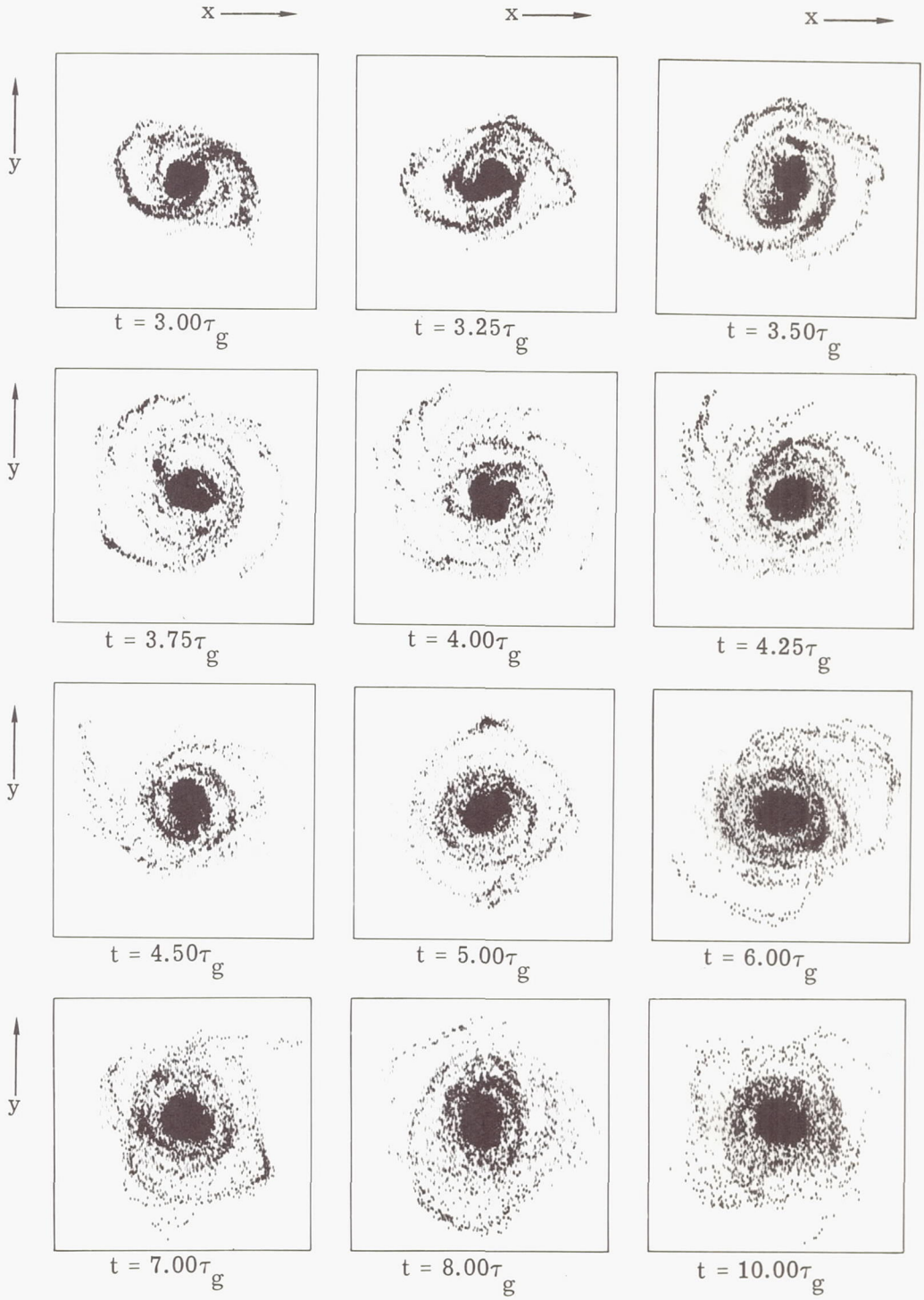

(b) Evolution up to $t = 10.00\tau_g$.

Figure 6.- Concluded.

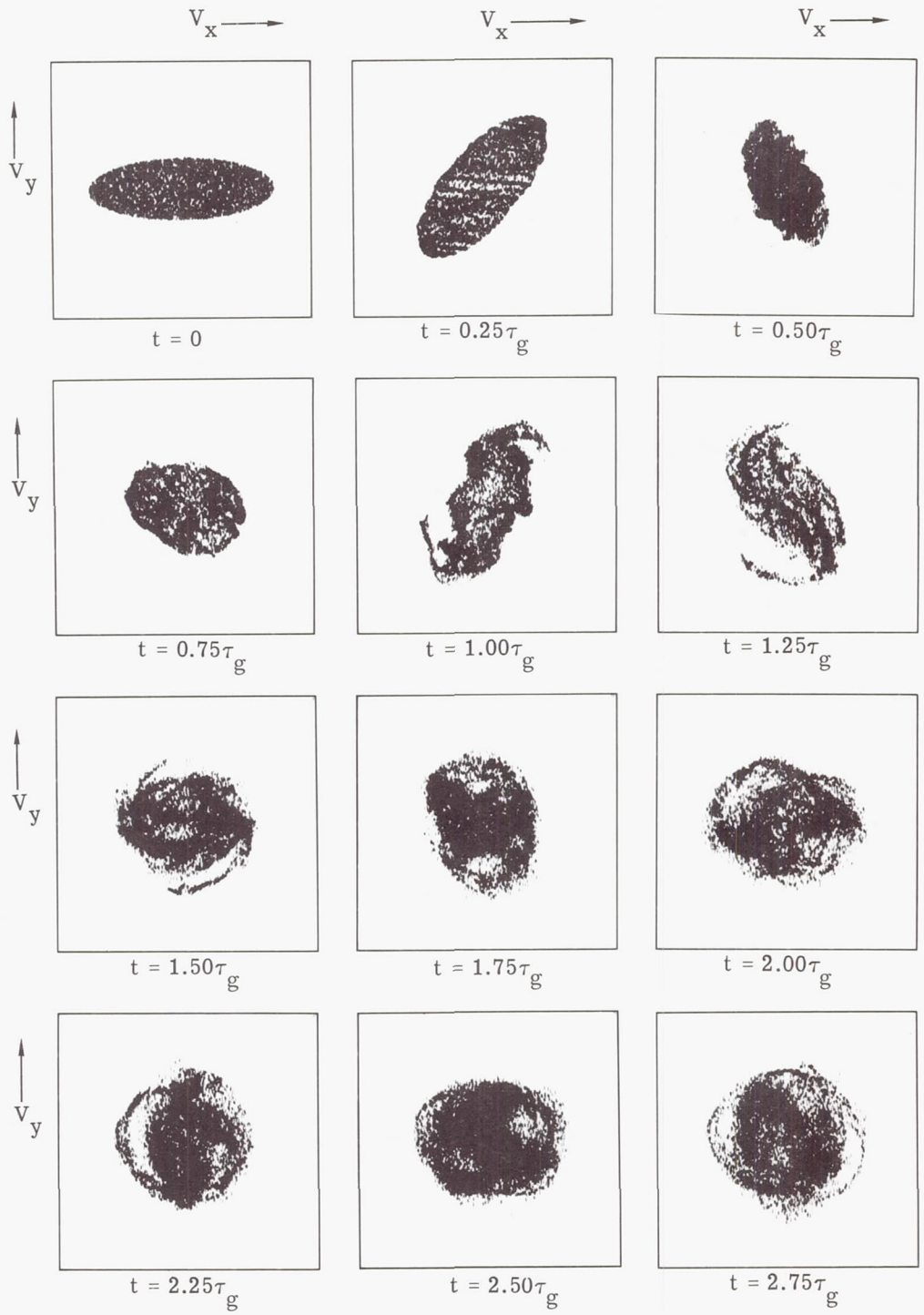

(a) Evolution up to $t = 2.75\tau_g$.

Figure 7.- Evolution of a 10 000-star system in V_x,V_y-velocity space.

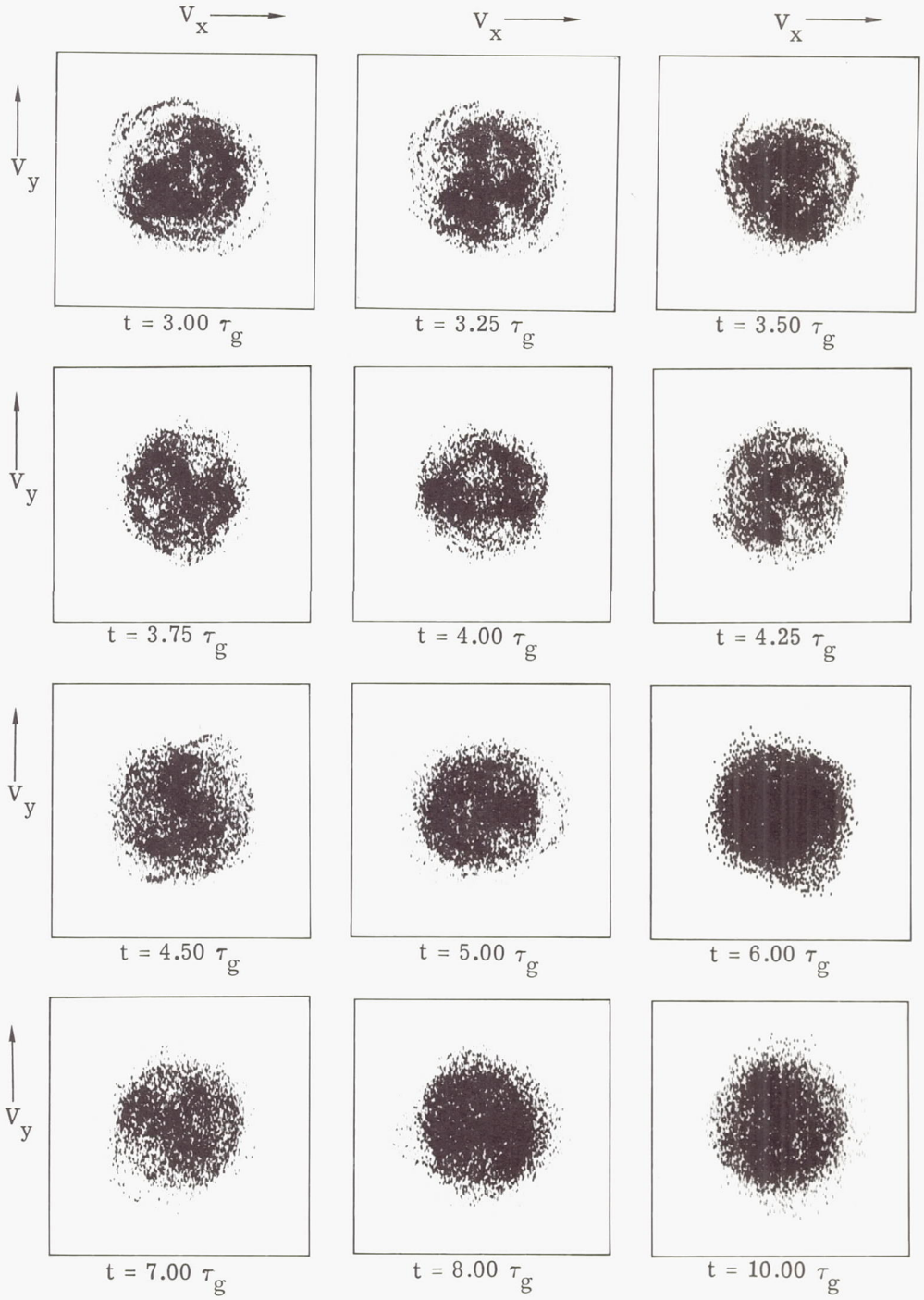

(b) Evolution up to $t = 10.00\tau_g$.

Figure 7.- Concluded.

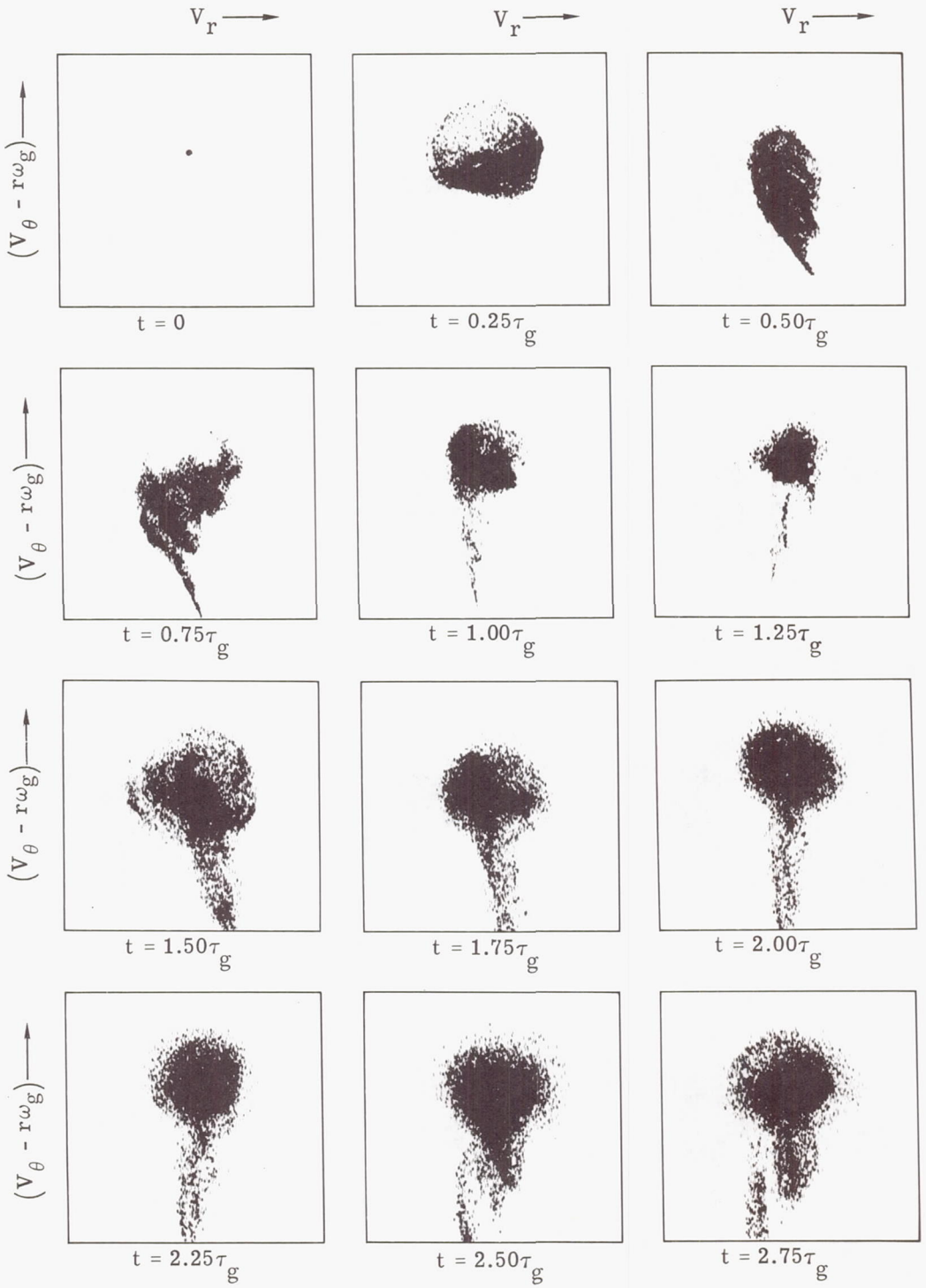

(a) Evolution up to $t = 2.75\tau_g$.

Figure 8.- Evolution of a 10 000-star system in $(V_\theta - r\omega_g)$,V_r-velocity space.

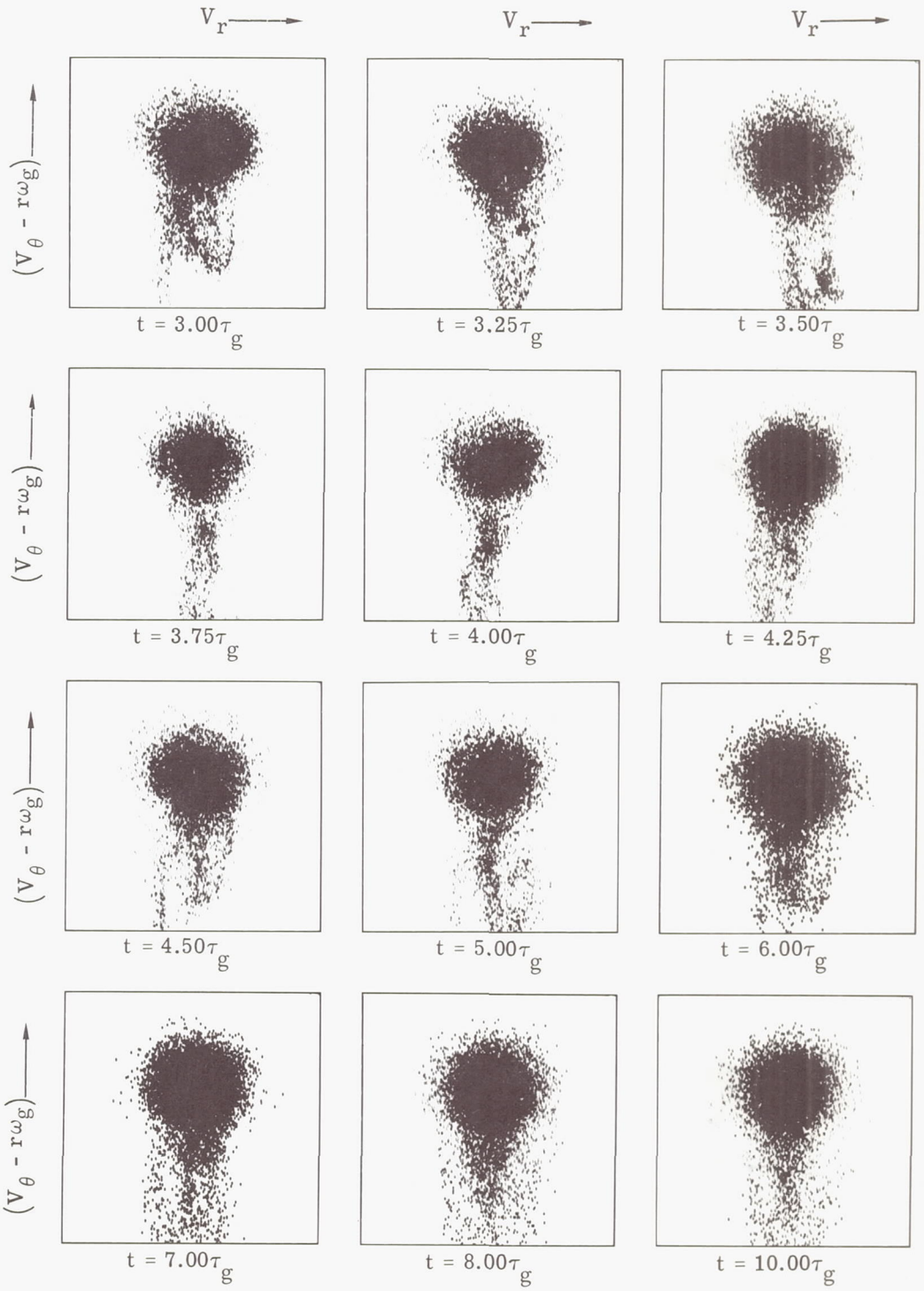

(b) Evolution up to $t = 10.00\tau_g$.

Figure 8.- Concluded.

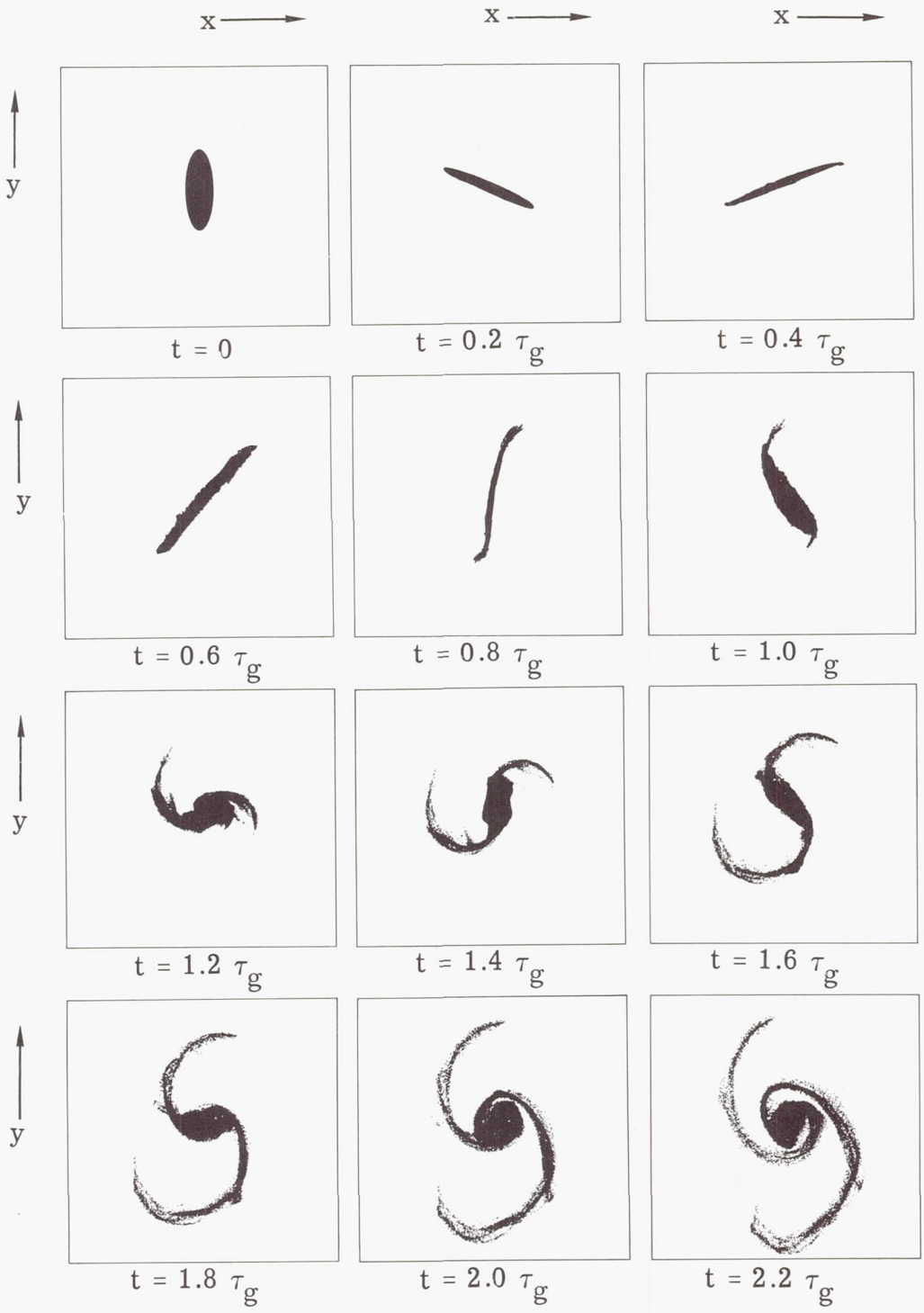

(a) Evolution up to $t = 2.2\tau_g$.

Figure 9.- Evolution of a 100 000-star system in x,y-coordinate space.

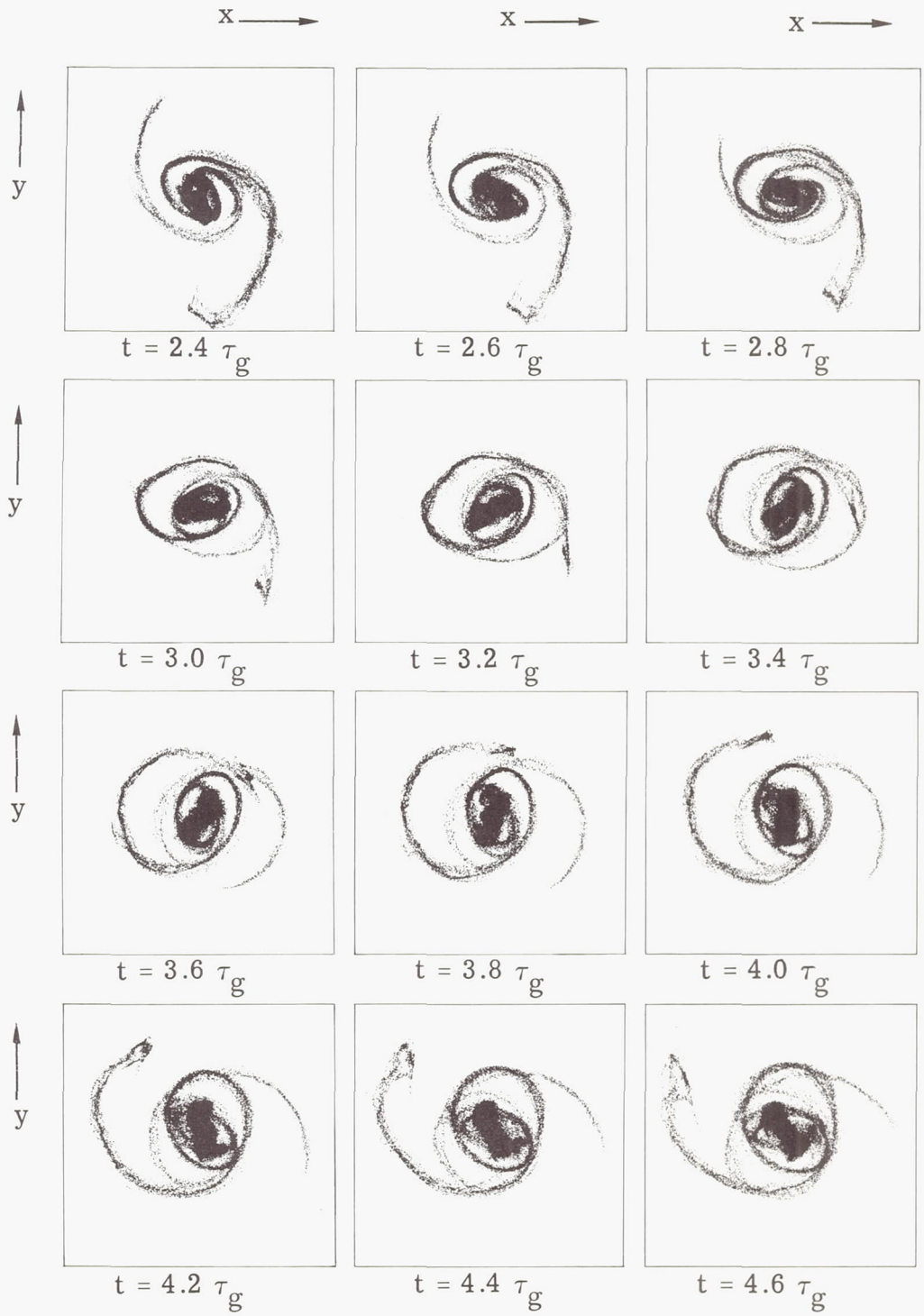

(b) Evolution up to $t = 4.6\tau_g$.

Figure 9.- Continued.

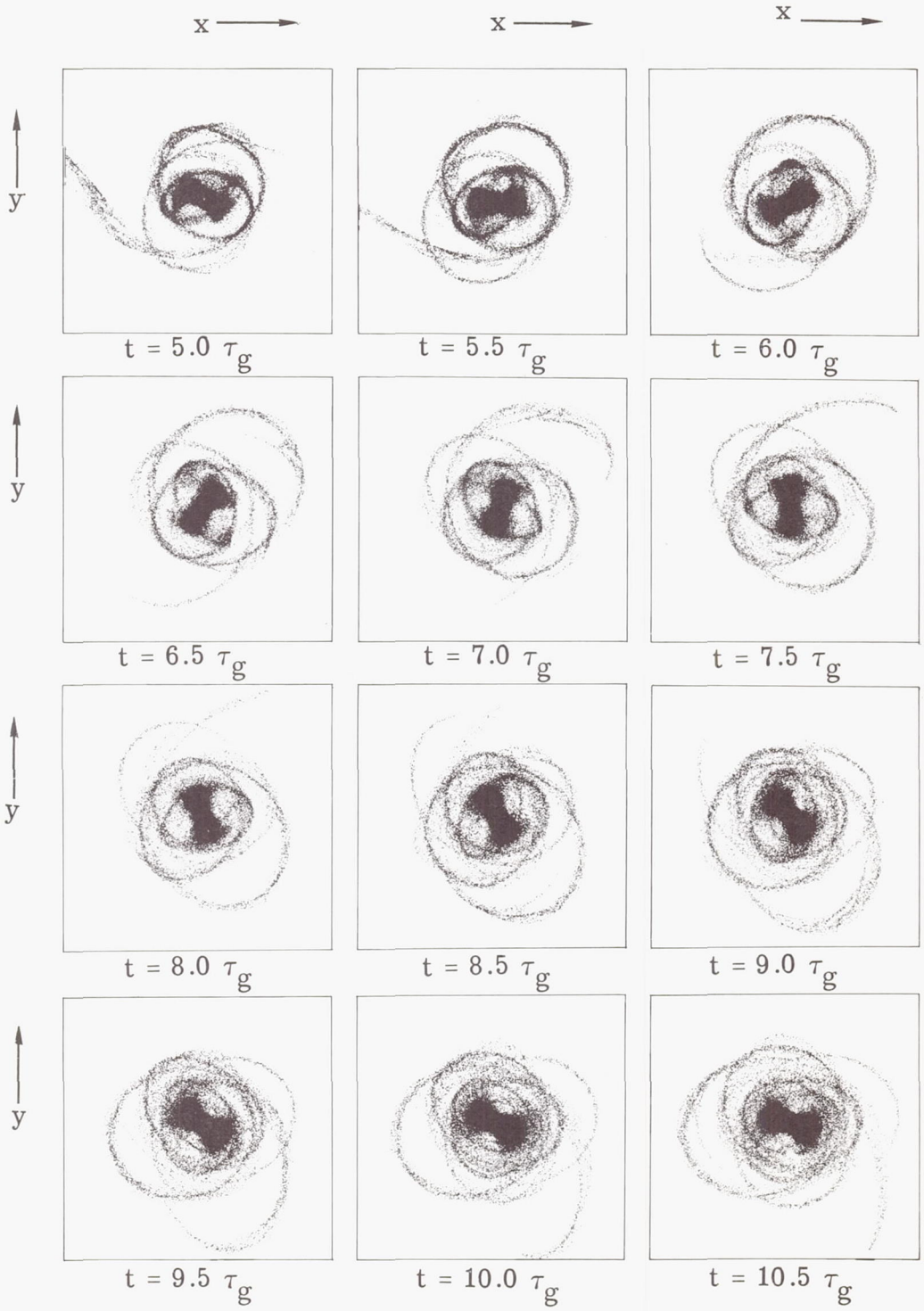

(c) Evolution up to $t = 10.5\tau_g$.

Figure 9.- Concluded.

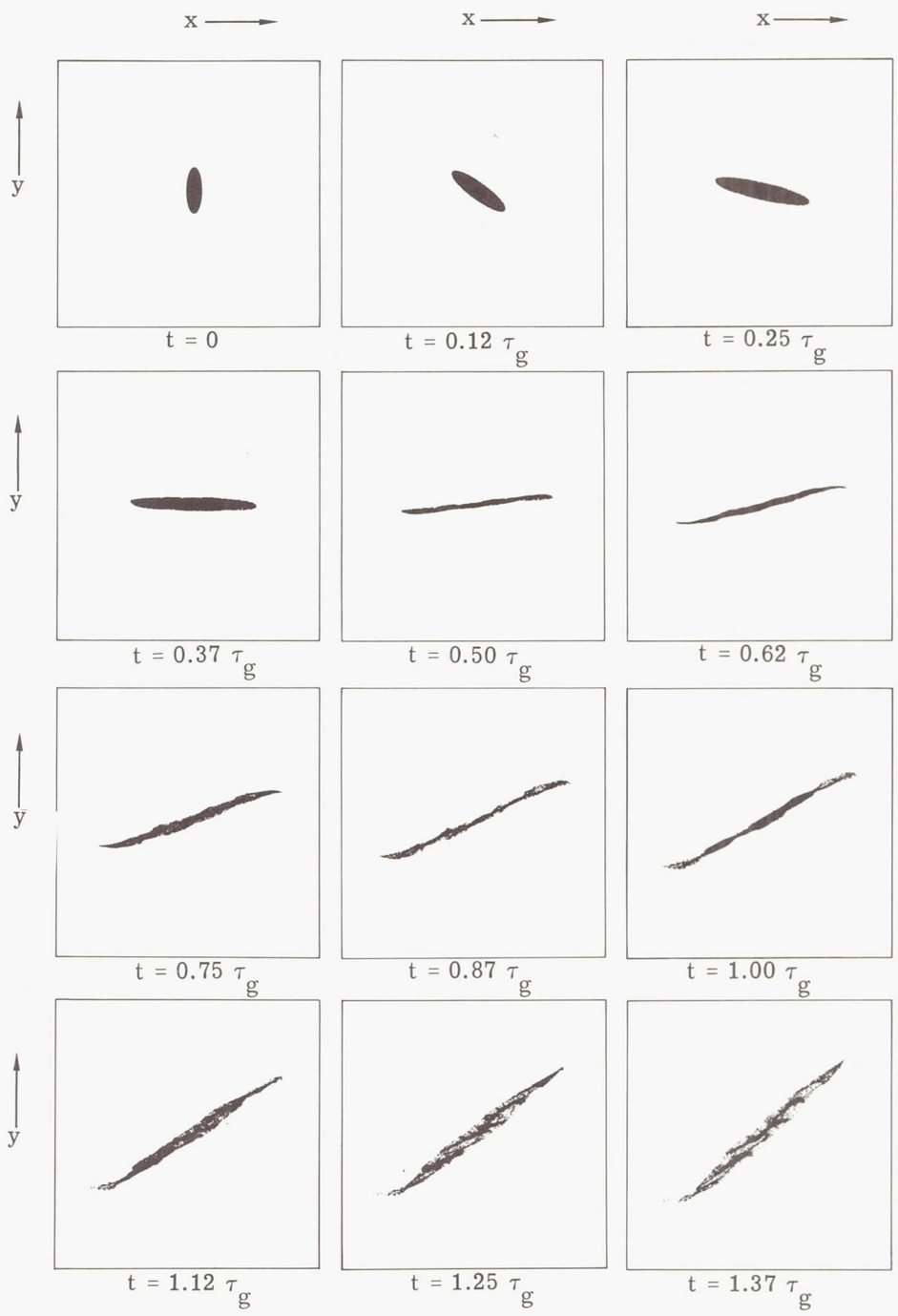

(a) Evolution up to $t = 1.37\tau_g$.

Figure 10.- Evolution in x,y-coordinate space of a 10 000-star system with an initial rotation equal to $1.3\omega_g$.

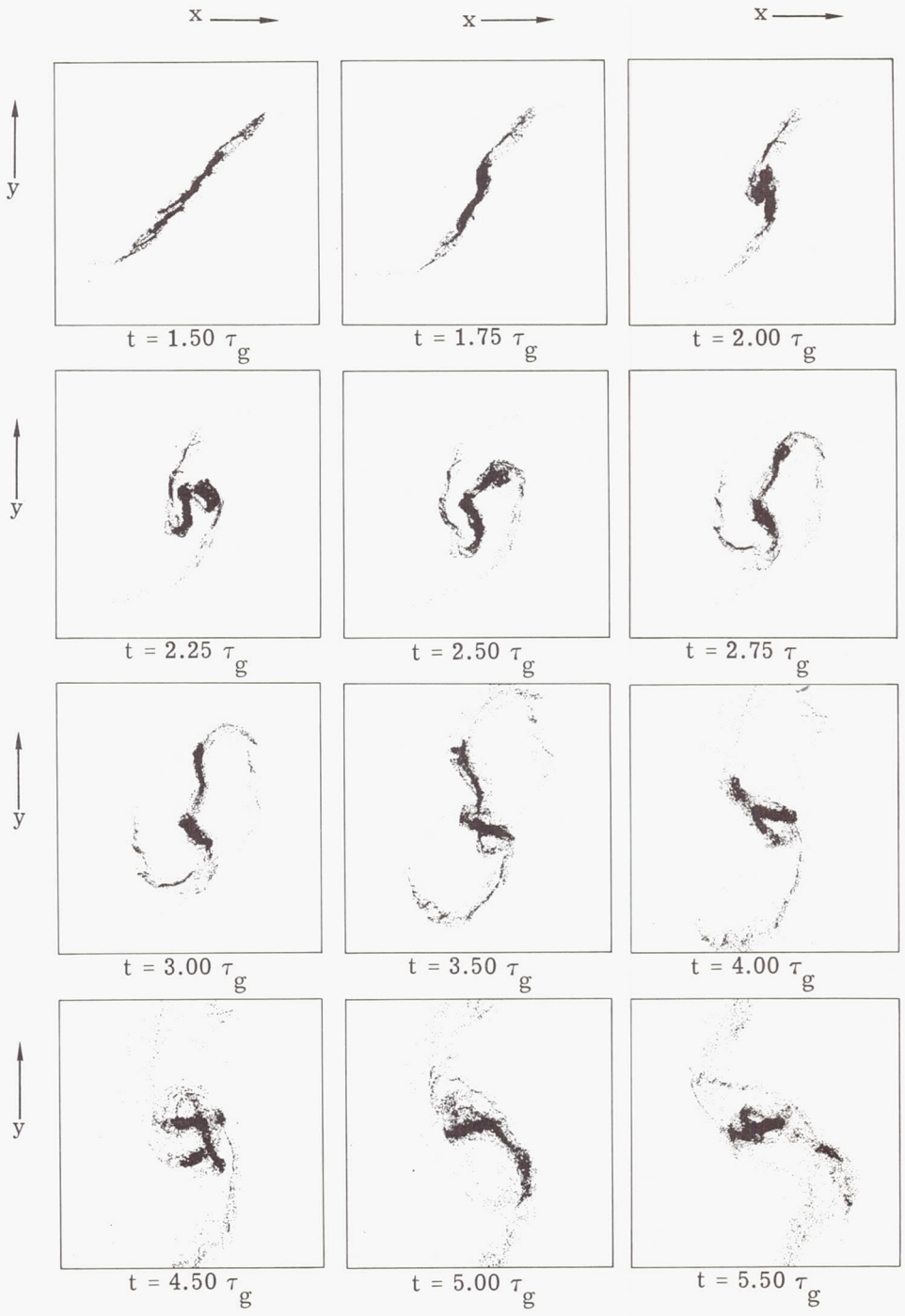

(b) Evolution up to $t = 5.5\tau_g$.

Figure 10.- Continued.

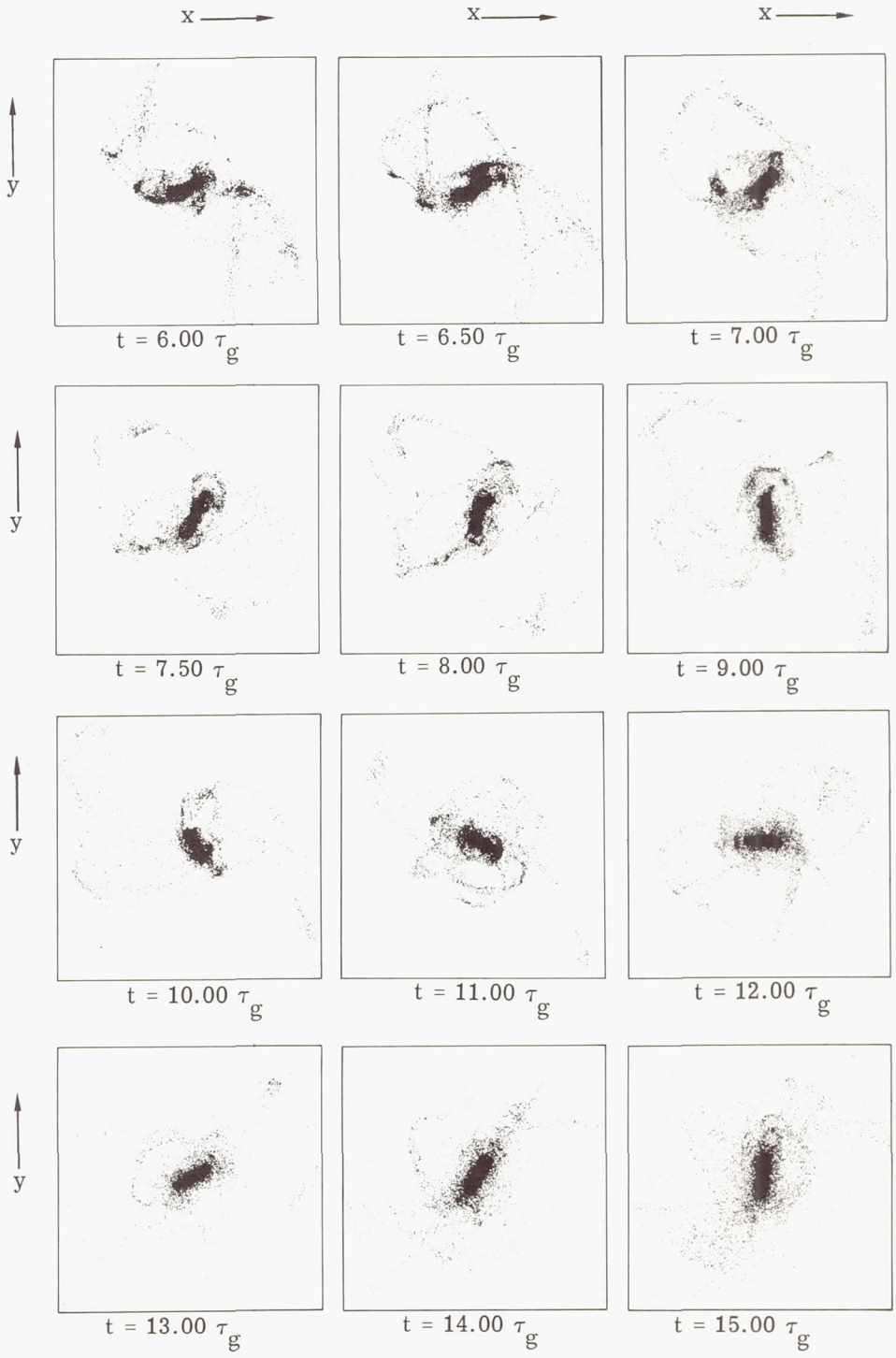

(c) Evolution up to $t = 15\tau_g$.

Figure 10.- Concluded.

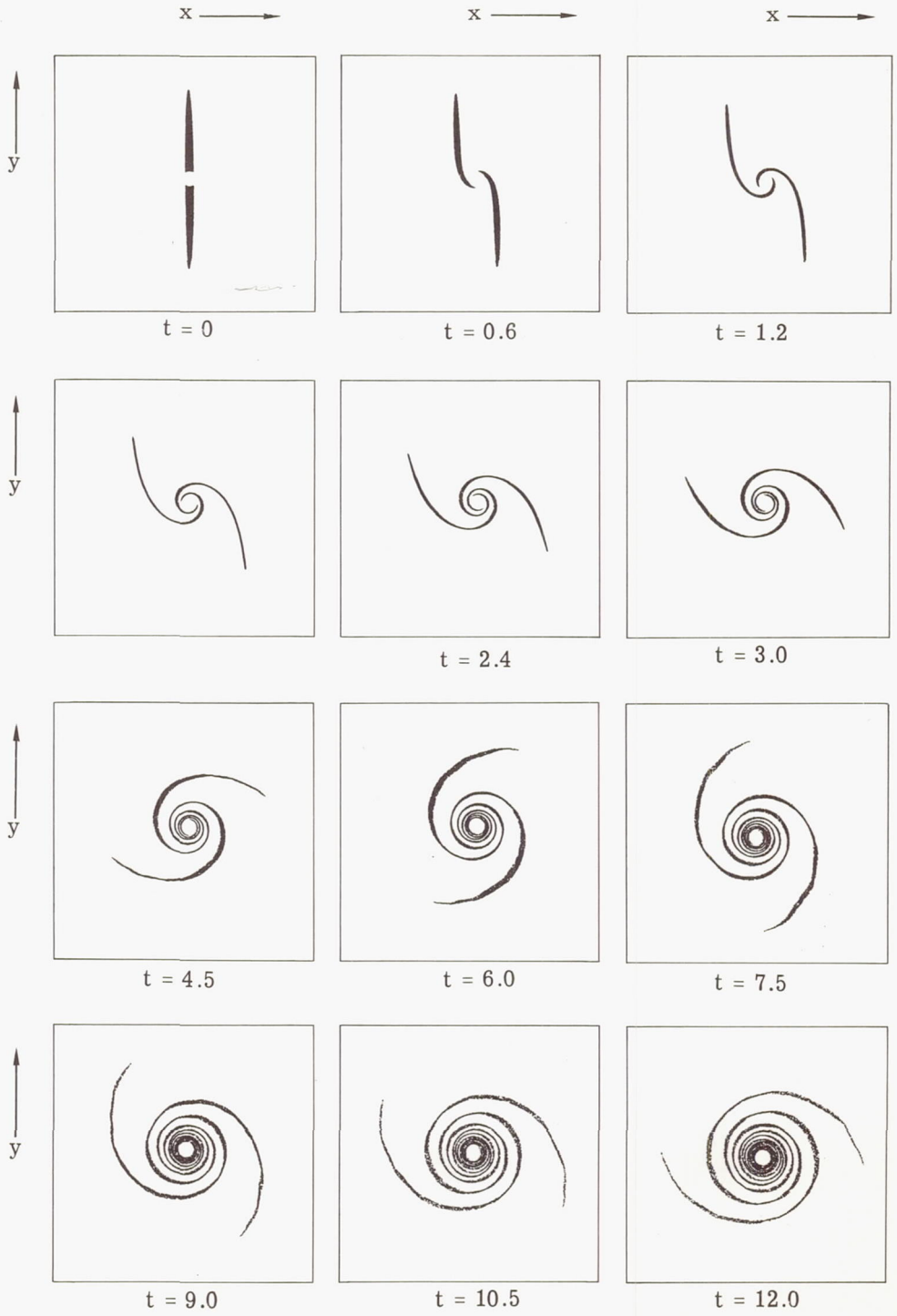

(a) Evolution up to t = 12.

Figure 11.- Evolution of a 10 000-star system in the presence of a large central mass equal to 10 times the mass of the 10 000 stars.

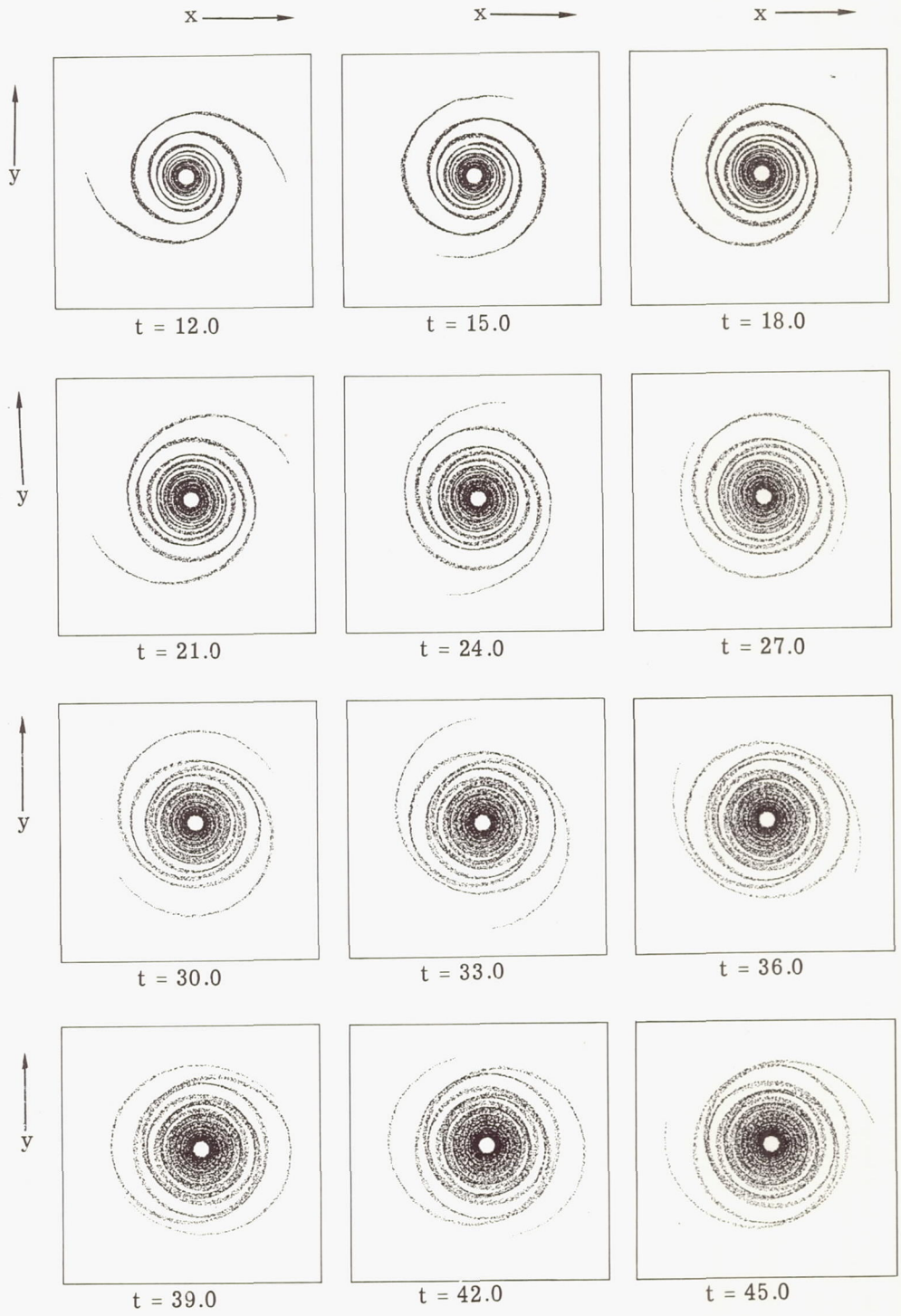

(b) Evolution up to t = 45.

Figure 11.- Concluded.

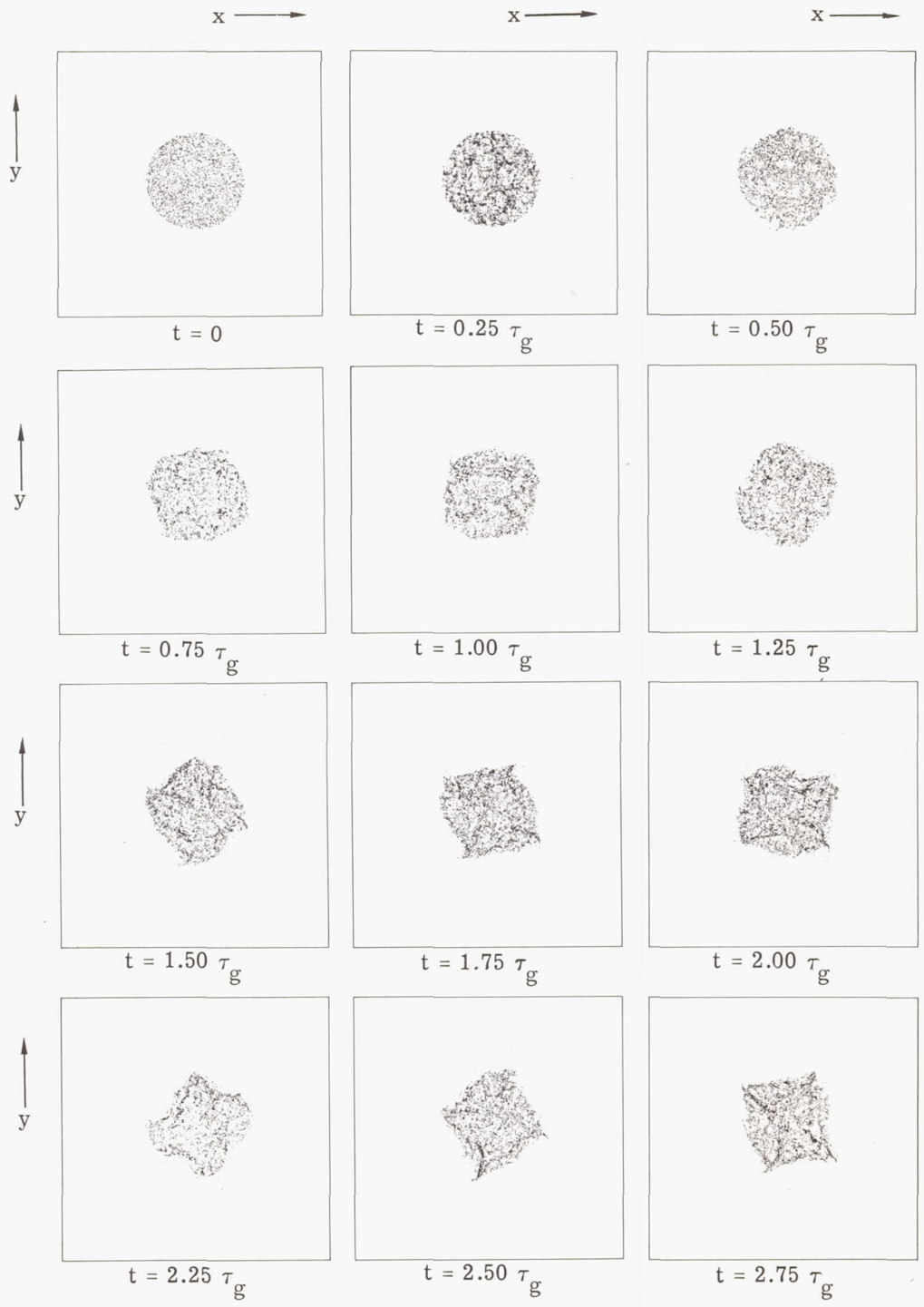

(a) Evolution up to $t = 2.75\tau_g$.

Figure 12.- Evolution of a 10 000-star system in x,y-coordinate space. The initial solid-body rotation of the system equaled that required to balance the gravitational attraction.

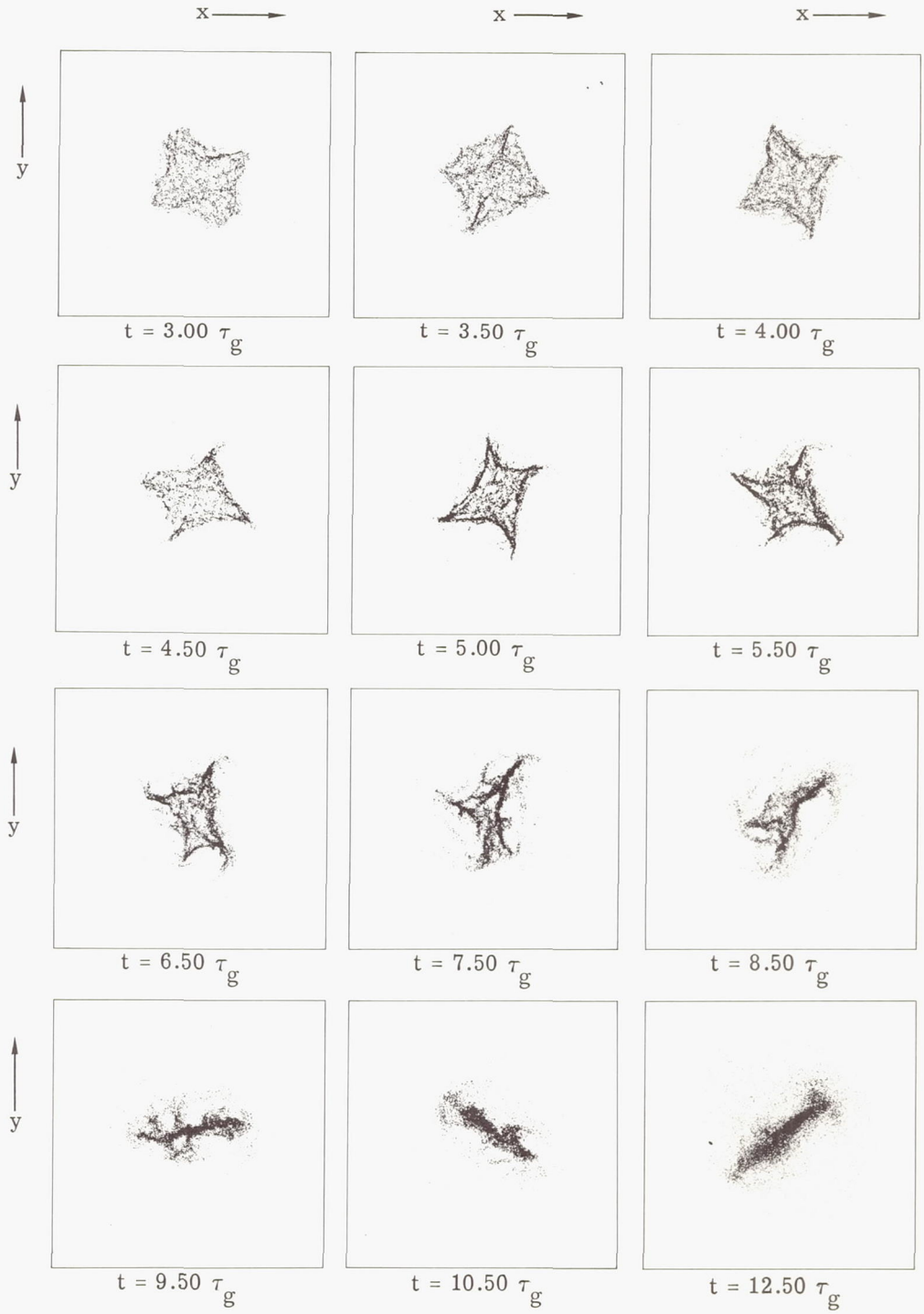

(b) Evolution up to $t = 12.5\tau_g$.

Figure 12.- Concluded.

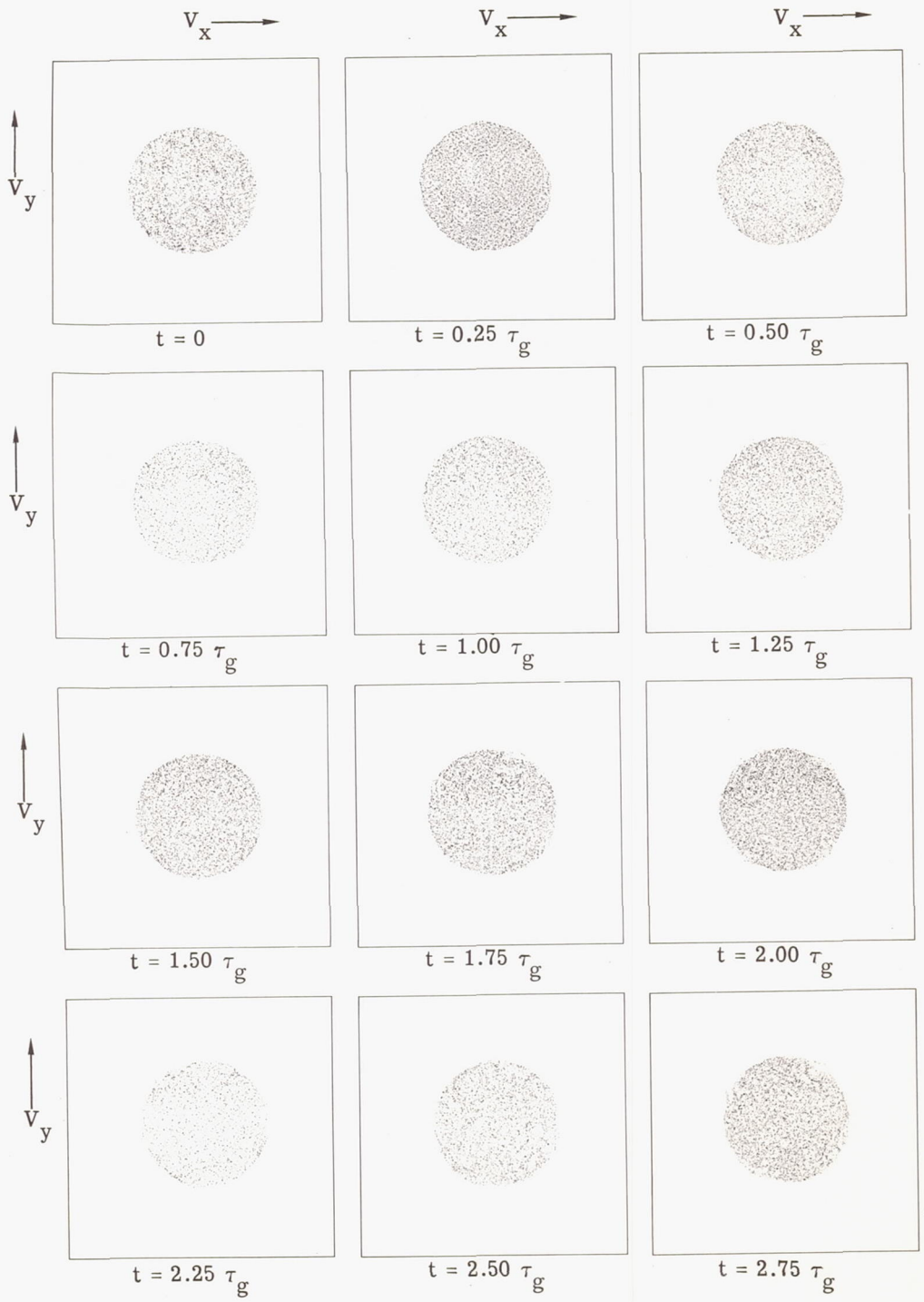

(a) Evolution up to $t = 2.75\tau_g$.

Figure 13.- Evolution of a 10 000-star system in V_X,V_Y-velocity space where initially the centrifugal force balances the gravitational attraction.

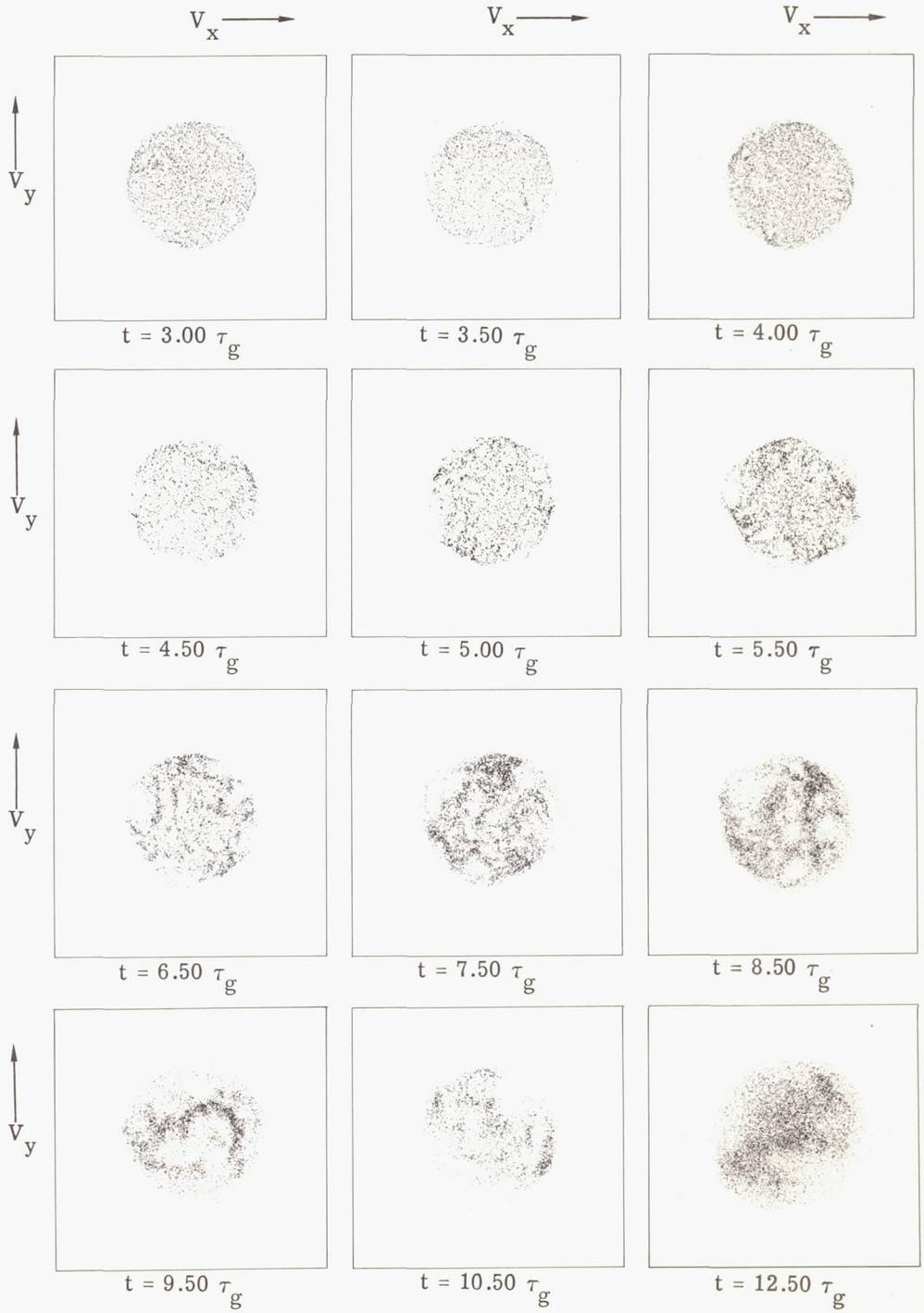

(b) Evolution up to $t = 12.5\tau_g$.

Figure 13.- Concluded.

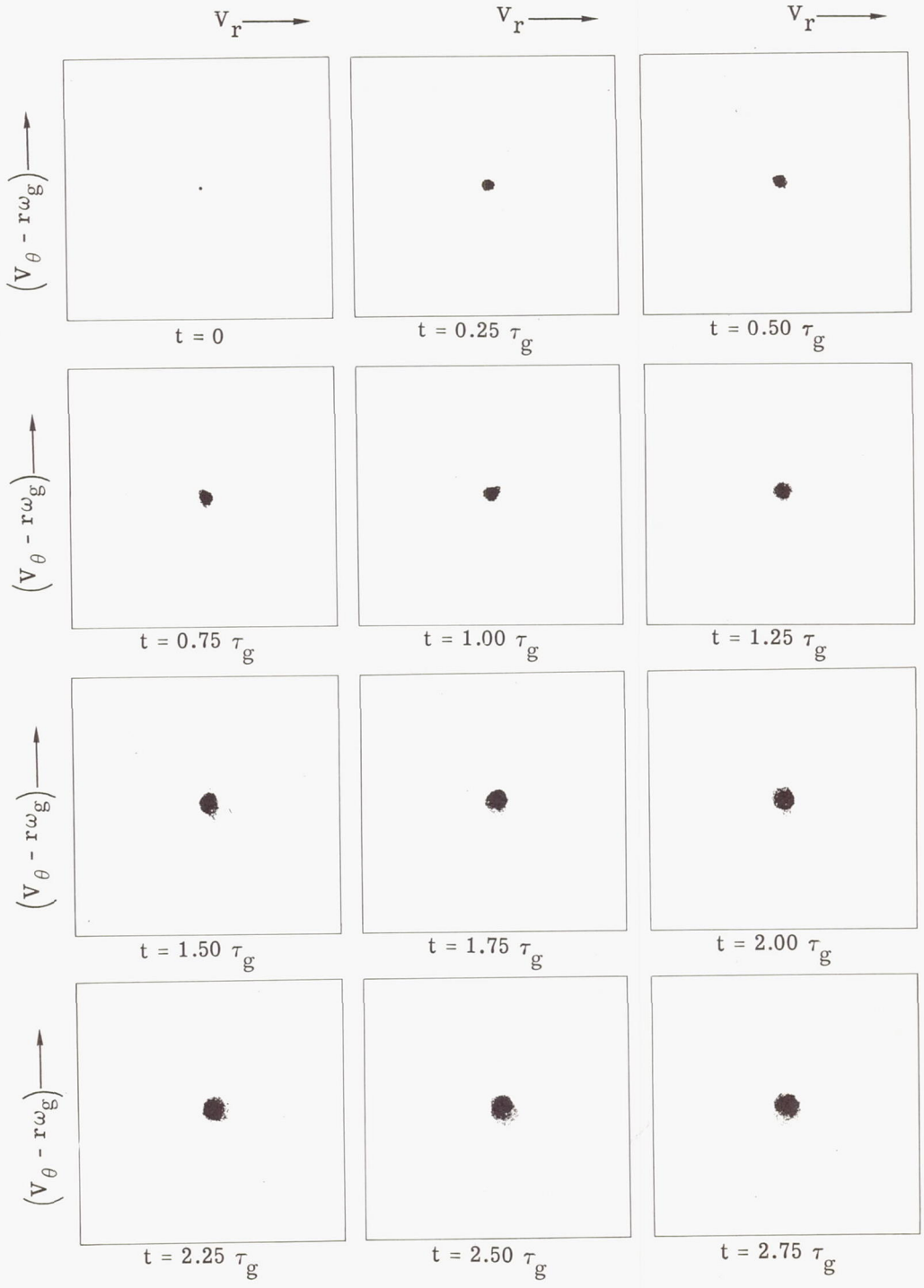

(a) Evolution up to $t = 2.75\tau_g$.

Figure 14.- Evolution of a 10 000-star system in V_r,$(V_\theta - r\omega_g)$-velocity space. The initial solid body rotation of the system equaled that required to balance the gravitational attraction.

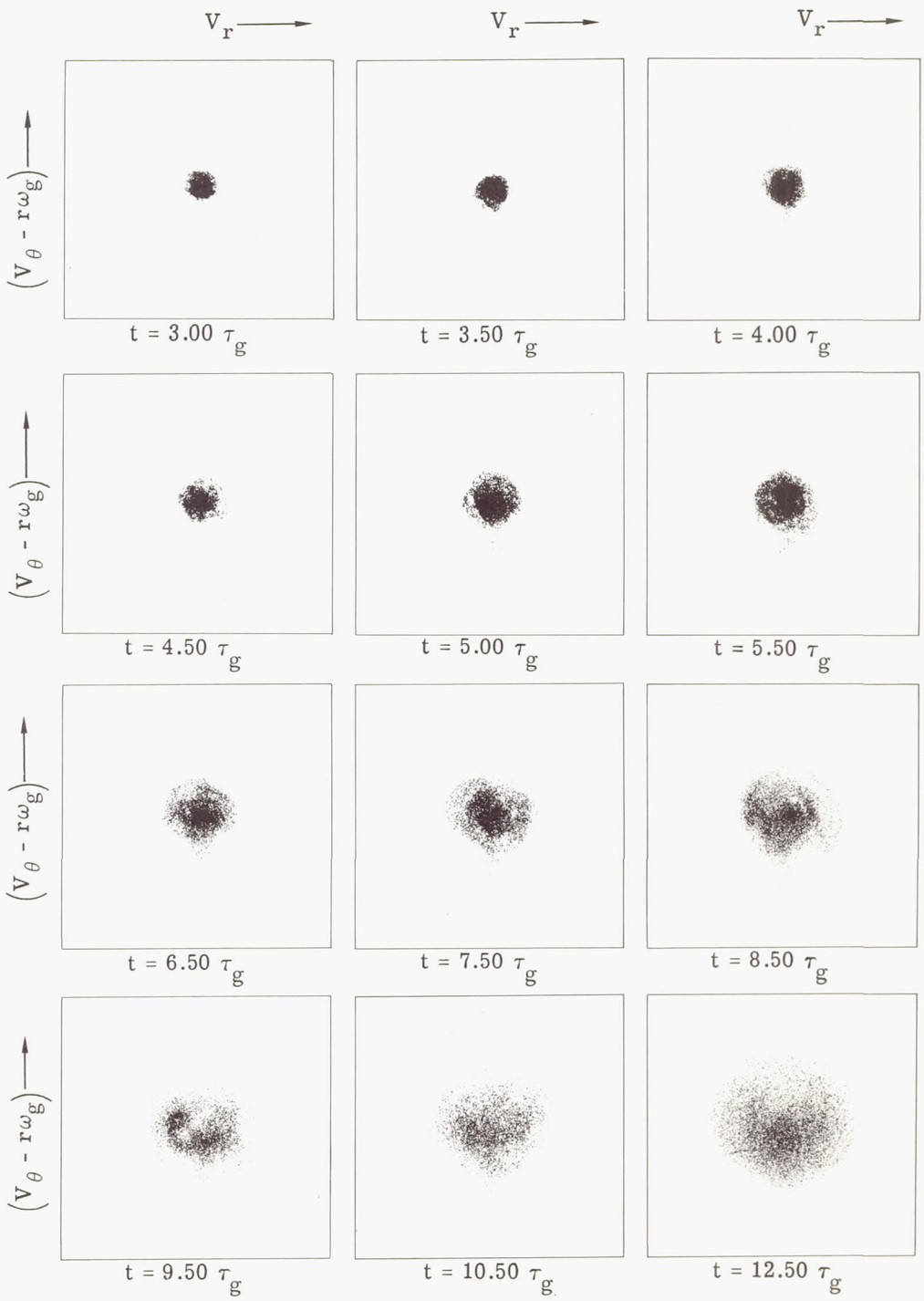

(b) Evolution up to $t = 12.5\tau_g$.

Figure 14.- Concluded.

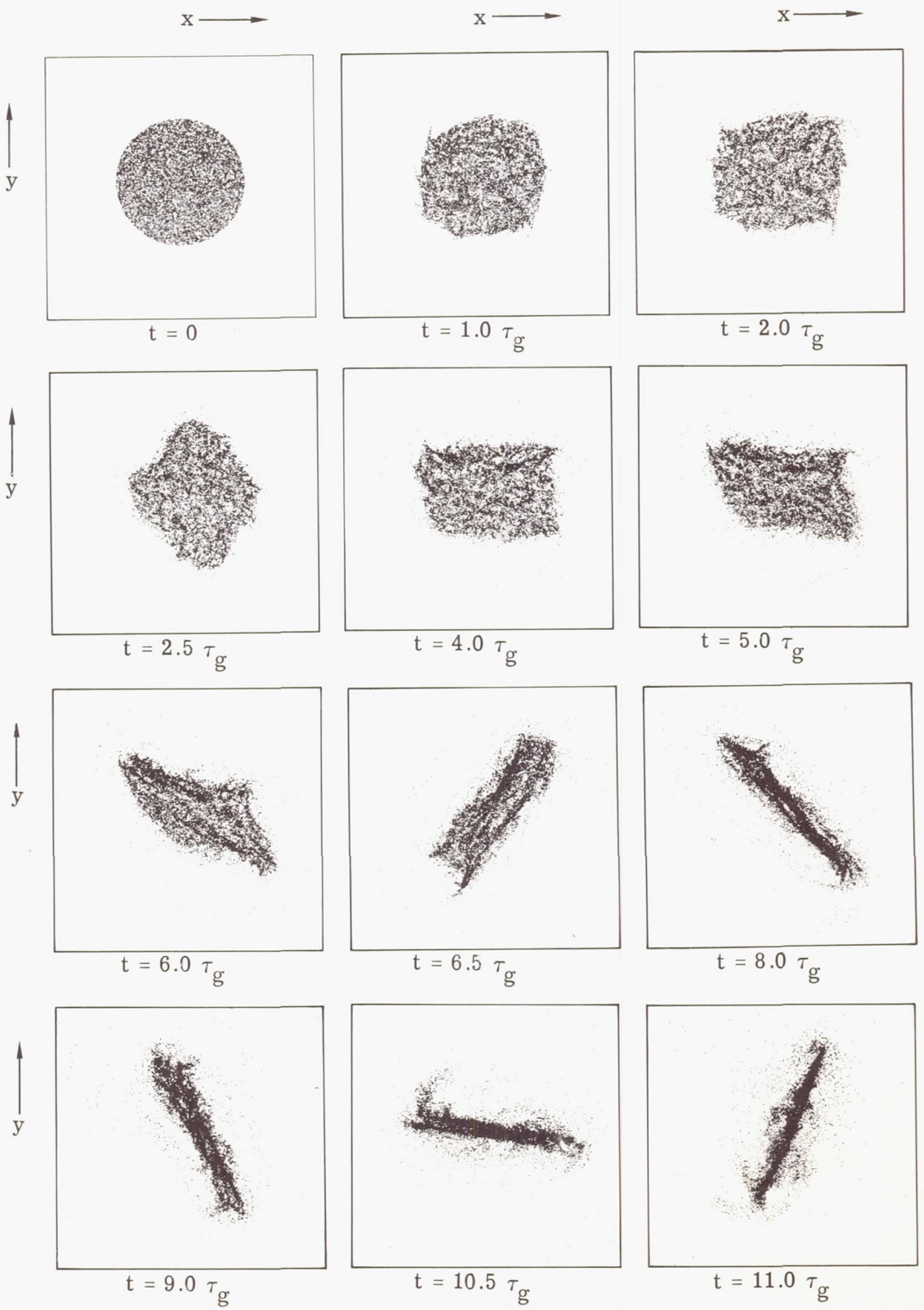

Figure 15.- Evolution of a balanced system like that shown in figure 12, but with a different pseudo-random number sequence for the initial star positions.

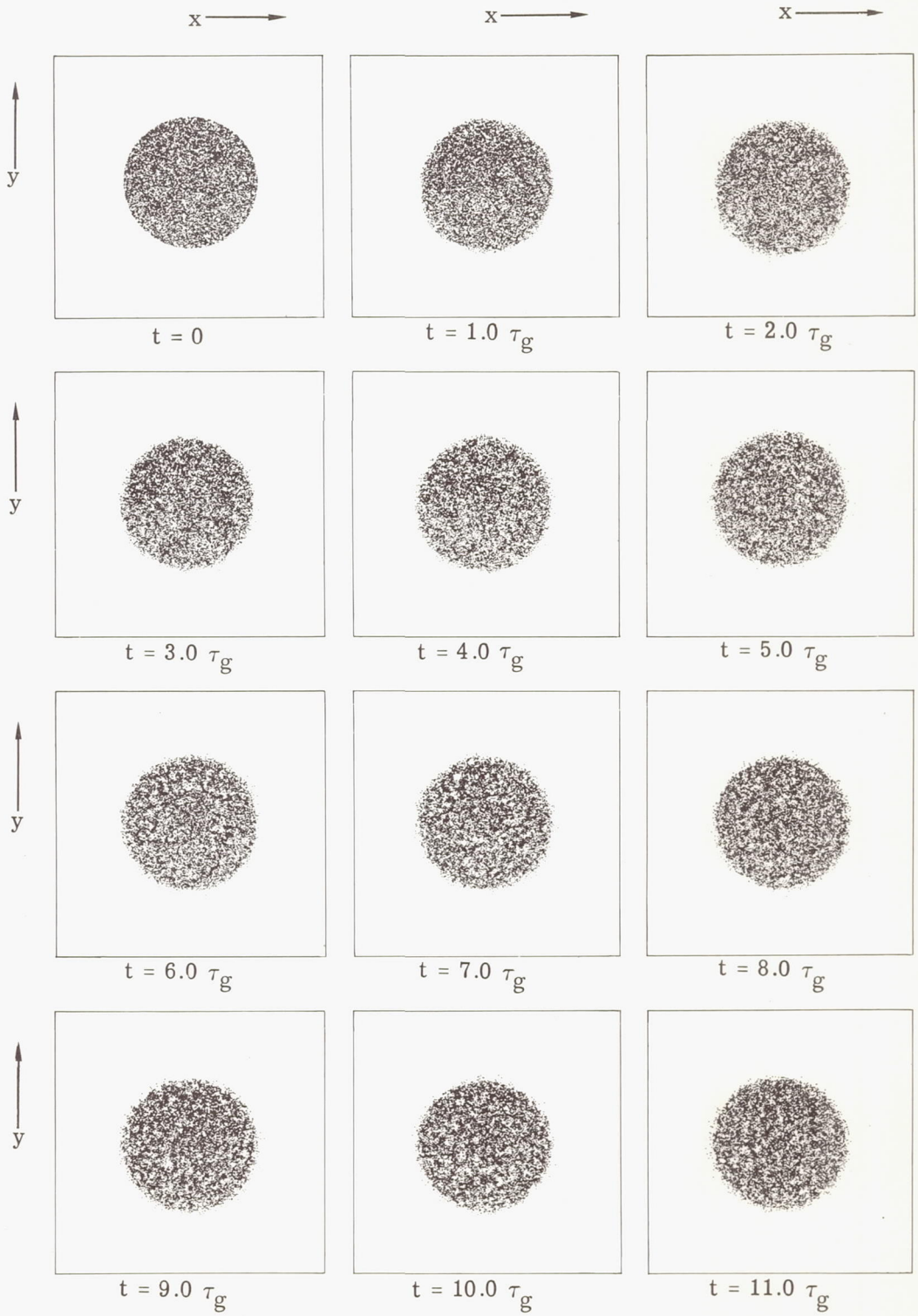

Figure 16.- Evolution of a balanced system with 5000 stars rotating clockwise and 5000 stars rotating counterclockwise.

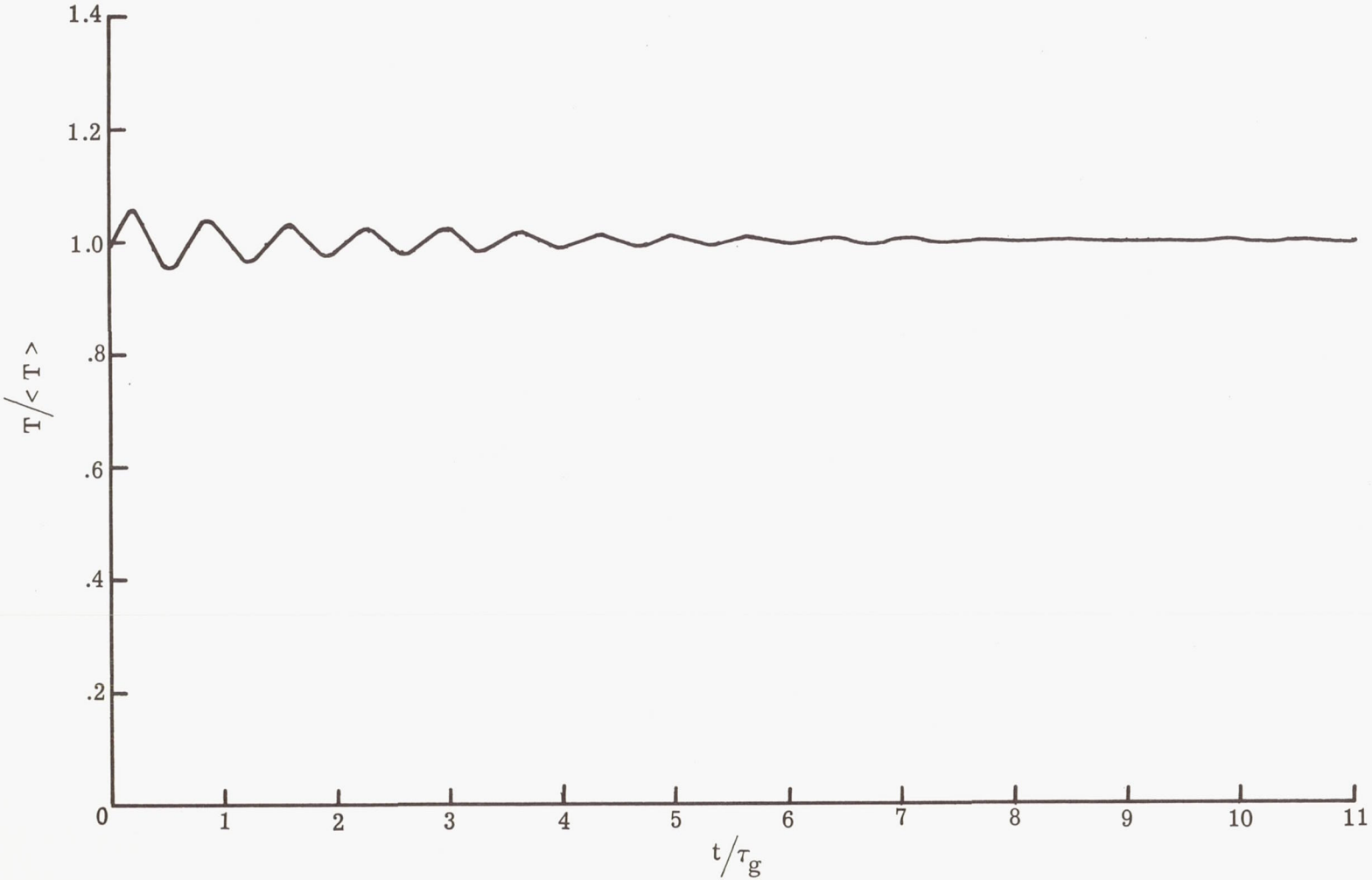

Figure 17.- Evolution in time of the kinetic energy for the balanced cylinder shown in figure 16.

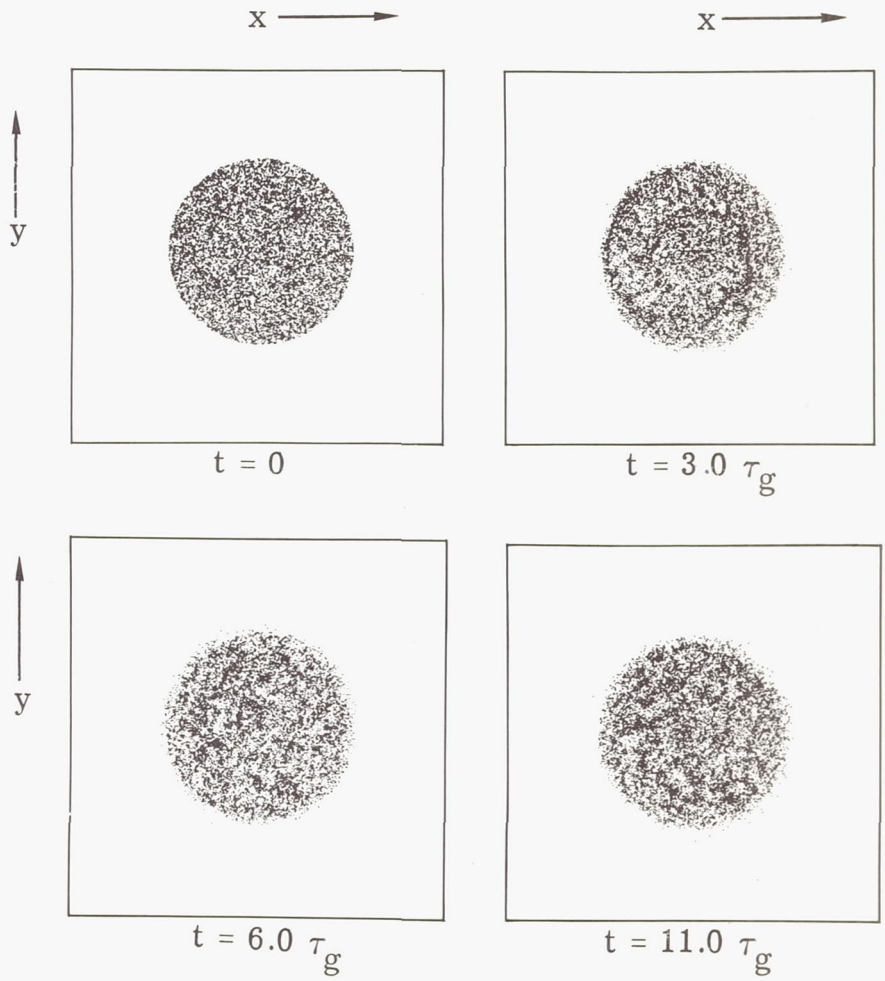

Figure 18.- Evolution in x,y-coordinate space for a stable system with counterrotating stars of different mass.

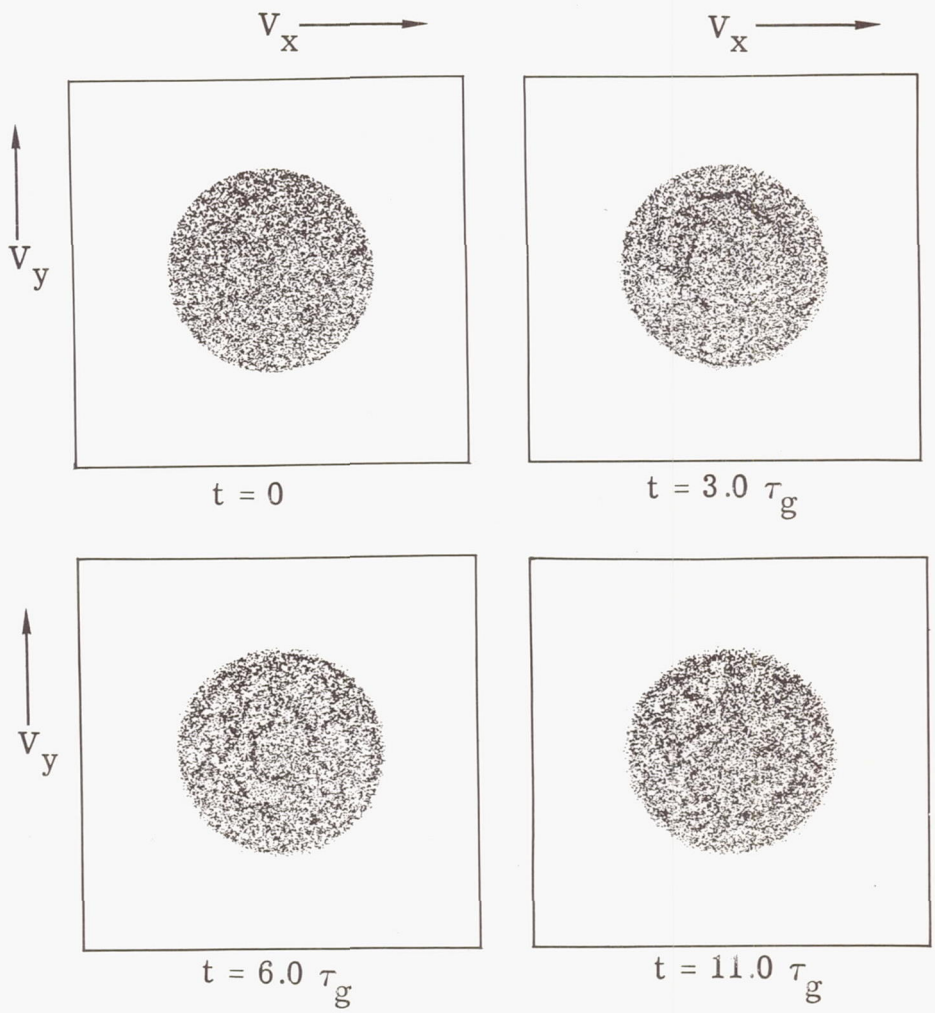

Figure 19.- Evolution of a stable system of counterrotating stars in V_x,V_y-velocity space.

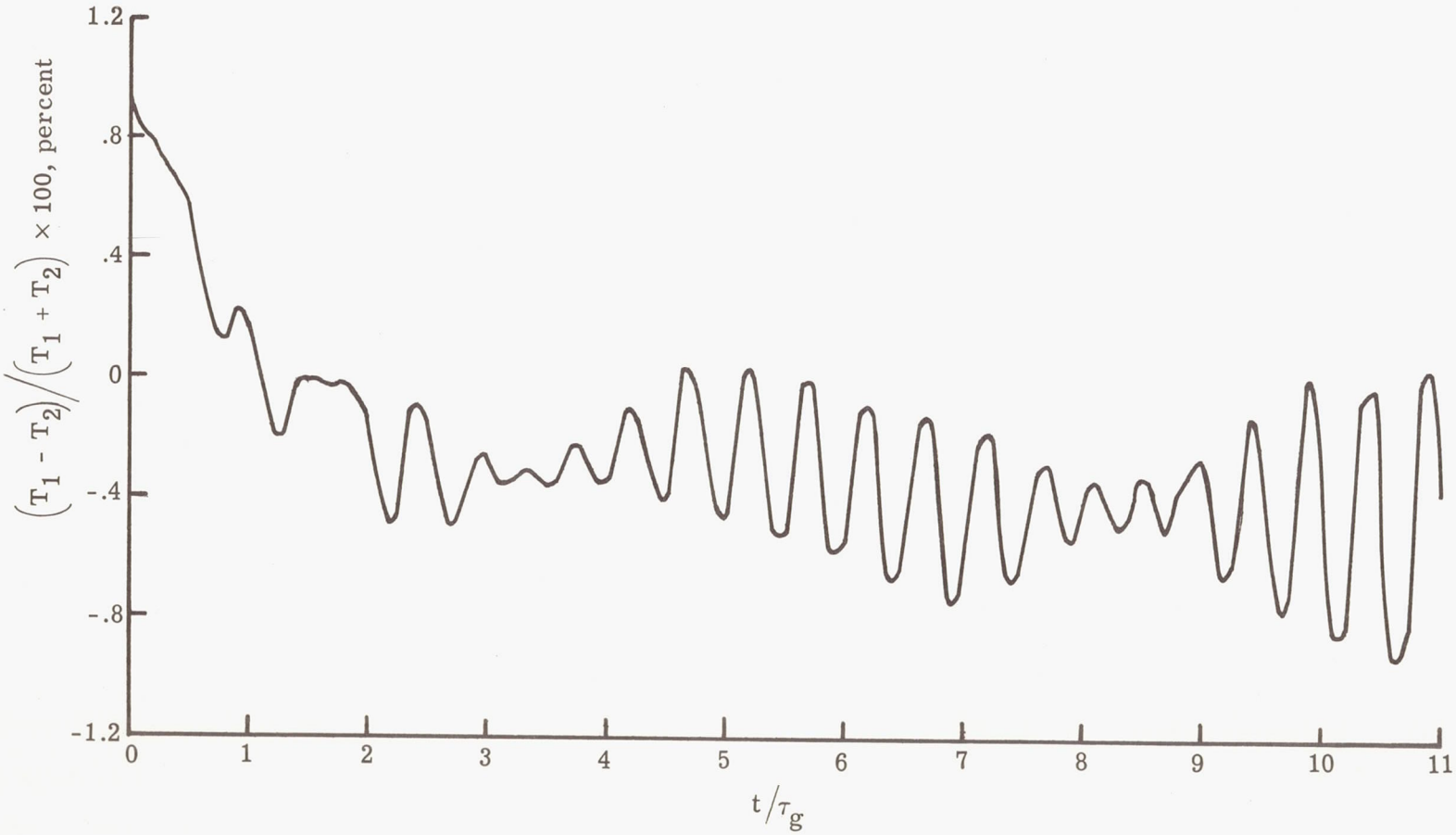

Figure 20.- Rate at which equipartition of energy occurs for a stable system containing 5000 stars of mass m/2 and 5000 stars of mass 3m/2.